Article

SOURCE DATA

EMBO reports

HDAC6 deacetylates IDH1 to promote the homeostasis of hematopoietic stem and progenitor cells

Jia Yang[1,†], Yang Liu[1,†], Hanxiao Yin[1,†], Songbo Xie[2], Linlin Zhang[1], Xifeng Dong[3], Hua Ni[1], Weiwen Bu[1], Hongbo Ma[1], Peng Liu[4], Haiyan Zhu[4], Rongxia Guo[4], Lei Sun[2], Yue Wu[2], Juan Qin[1], Baofa Sun[1], Dengwen Li[1], Hongbo R Luo[5], Min Liu[6,*], Chenghao Xuan[7,**] & Jun Zhou[1,2,***]

Abstract

Hematopoietic stem and progenitor cells (HSPCs) are cells mainly present in the bone marrow and capable of forming mature blood cells. However, the epigenetic mechanisms governing the homeostasis of HSPCs remain elusive. Here, we demonstrate an important role for histone deacetylase 6 (HDAC6) in regulating this process. Our data show that the percentage of HSPCs in *Hdac6* knockout mice is lower than in wild-type mice due to decreased HSPC proliferation. HDAC6 interacts with isocitrate dehydrogenase 1 (IDH1) and deacetylates IDH1 at lysine 233. The deacetylation of IDH1 inhibits its catalytic activity and thereby decreases the 5-hydroxymethylcytosine level of ten-eleven translocation 2 (TET2) target genes, changing gene expression patterns to promote the proliferation of HSPCs. These findings uncover a role for HDAC6 and IDH1 in regulating the homeostasis of HSPCs and may have implications for the treatment of hematological diseases.

Keywords 5-hydroxymethylcytosine; cell proliferation; HDAC6; HSPCs; IDH1
Subject Categories Chromatin, Transcription, & Genomics; Post-translational Modifications & Proteolysis; Stem Cells & Regenerative Medicine
DOI 10.15252/embr.202256009 | Received 23 August 2022 | Revised 27 July 2023 | Accepted 14 August 2023 | Published online 29 August 2023
EMBO Reports (2023) 24: e56009

Introduction

Hematopoietic stem and progenitor cells (HSPCs) are cells that reside primarily in the bone marrow and possess self-renewal and differentiation capacities (Laurenti & Gottgens, 2018; Wilkinson *et al*, 2020; Ferrari *et al*, 2021). The homeostasis of HSPCs is regulated by orderly cell proliferation, differentiation, and apoptosis, and is necessary for hematopoiesis, a process by which the body manufactures blood cells (Laurenti & Gottgens, 2018; Rasheed, 2022). There is compelling evidence that epigenetic modification is essential for regulating the homeostasis of HSPCs. For example, the level of DNA methylation has profound effects on hematopoietic cell fate determination; *Dnmt3a* knockout hematopoietic stem cells (HSCs) exhibit enhanced self-renewal capacity and a predisposition for the erythroid differentiation program (Challen *et al*, 2011; Izzo *et al*, 2020), while ten-eleven translocation 2 (*Tet2*) knockout HSCs present elevated self-renewal ability and a slanted myelomonocytic differentiation (Ko *et al*, 2011; Moran-Crusio *et al*, 2011; Quivoron *et al*, 2011). Interestingly, double knockout of *Dnmt3a* and *Tet2* leads to a more severe and complex phenotype in the hematopoietic system (Zhang *et al*, 2016). Epigenetic dysregulation has been implicated in a variety of hematological diseases, including myeloproliferative diseases and loss of immune function (Ntziachristos *et al*, 2016).

Histone acetylation is another epigenetic modification that participates in the homeostasis of HSPCs and is regulated by two types of enzymes, histone acetyltransferases and histone deacetylases

1 State Key Laboratory of Medicinal Chemical Biology, Haihe Laboratory of Cell Ecosystem, Tianjin Key Laboratory of Protein Science, College of Life Sciences, Nankai University, Tianjin, China
2 Center for Cell Structure and Function, College of Life Sciences, Shandong Provincial Key Laboratory of Animal Resistance Biology, Collaborative Innovation Center of Cell Biology in Universities of Shandong, Shandong Normal University, Jinan, China
3 Department of Hematology, Tianjin Medical University General Hospital, Tianjin, China
4 State Key Laboratory of Experimental Hematology, Institute of Hematology and Blood Diseases Hospital, Chinese Academy of Medical Sciences and Peking Union Medical College, Tianjin, China
5 Department of Pathology, Department of Laboratory Medicine, Harvard Medical School, Children's Hospital Boston, Dana-Farber/Harvard Cancer Center, Boston, MA, USA
6 Laboratory of Tissue Homeostasis, Haihe Laboratory of Cell Ecosystem, Tianjin, China
7 The Province and Ministry Co-sponsored Collaborative Innovation Center for Medical Epigenetics, Key Laboratory of Immune Microenvironment and Disease of the Ministry of Education, Department of Biochemistry and Molecular Biology, School of Basic Medical Sciences, Tianjin Medical University, Tianjin, China
*Corresponding author. Tel: +86 22 2350 4946; Fax: +86 22 2350 4946; E-mail: minliu@nankai.edu.cn
**Corresponding author. Tel: +86 22 8333 6995; Fax: +86 22 8333 6995; E-mail: chenghaoxuan@tmu.edu.cn
***Corresponding author. Tel: +86 22 2349 4816; Fax: +86 22 2349 4816; E-mail: junzhou@nankai.edu.cn
†These authors contributed equally to this work

(HDACs; Jiang *et al*, 2019; Rodrigues *et al*, 2020). These enzymes modulate the acetylation of core histones by adding or removing acetyl groups on the lysine residues, ultimately regulating chromatin accessibility (Neganova *et al*, 2022). In addition to histones, the substrates of HDACs include non-histone proteins. For example, HDAC6, a class IIb family member of HDACs, can deacetylate a number of cytoplasmic proteins such as α-tubulin and cortactin, thereby regulating cell motility, ciliary homeostasis, virus infection, immunity, and many other cellular processes (Hubbert *et al*, 2002; Zhang *et al*, 2003, 2007, 2015; Valenzuela-Fernandez *et al*, 2005; Huo *et al*, 2011; Ran *et al*, 2015, 2020, 2022; Wang *et al*, 2015; Yan *et al*, 2017, 2018; Xie *et al*, 2020). HDAC6 has also been shown to promote angiogenesis (Kaluza *et al*, 2011; Li *et al*, 2011), a process in which new blood vessels are formed from existing vessels. However, it remains elusive whether HDAC6 is involved in the regulation of hematopoiesis.

In this study, we investigated a potential role of HDAC6 in the hematopoietic system. We found that *Hdac6*-deficient mice had a significantly lower percentage of HSPCs than wild-type mice due to the decreased proliferation of HSPCs. Mechanistic experiments showed that HDAC6 deacetylates isocitrate dehydrogenase 1 (IDH1), a protein critically involved in the regulation of HSPC proliferation (Sasaki *et al*, 2012; Shi *et al*, 2015), and thereby reduces the enzyme activity of IDH1. The altered IDH1 enzymatic activity further decreased the level of 5-hydroxymethylcytosine (5hmC) in TET2 target genes, ultimately promoting the proliferation of HSPCs. As abnormal proliferation of HSPCs can lead to a wide spectrum of hematological diseases, our findings suggest that targeting HDAC6 may hold promise for the prevention and treatment of these diseases.

Results

Loss of HDAC6 impairs the proliferation of HSPCs in the bone marrow

The classic lineage of HSCs has been clearly classified in adult mouse bone marrow (Weissman, 2000; Mahadik *et al*, 2019). HSCs can be simply divided into long-term HSCs (LT-HSCs) with high self-renewal ability, and short-term HSCs (ST-HSCs) with limited self-renewal ability. ST-HSCs further differentiate into multipotent progenitor cells (MPPs). These three groups of cells are referred to as the LSK ($Lin^-c\text{-}Kit^+Sca1^+$) subsets, and have the potential for multi-lineage cell differentiation (Fig EV1A). MPPs further differentiate into uni-lineage progenitor cells, including common lymphoid progenitors (CLPs) and common myeloid progenitors (CMPs), which can only differentiate into lymphoid or myeloid cells, respectively. In addition, CMPs further differentiate into granulocyte/macrophage progenitors (GMPs) or megakaryocyte/erythroid progenitors (MEPs). Collectively, CMPs, GMPs, and MEPs are referred to as the LK ($Lin^-c\text{-}Kit^+Sca1^-$) subsets (Karatepe *et al*, 2018; Fig EV1A).

To determine whether HDAC6 regulates hemopoiesis, we obtained wild-type and *Hdac6* knockout mice (Fig 1A and B) and measured the number of blood cells in peripheral blood and hematopoietic cells in bone marrow. There was no significant difference between wild-type and *Hdac6* knockout mice in the number of total white blood cells or any blood cell lineage in the peripheral blood (Fig EV1B and D). In addition, no significant difference was found in the number of whole bone marrow cells between wild-type and *Hdac6* knockout mice (Fig 1C). However, the number and frequency of the LK cells slightly decreased, while the LSK cells in the bone marrow decreased significantly in *Hdac6* knockout mice (Fig 1D–F). We then examined the frequency and number of the LK subsets, including GMPs ($Lin^-c\text{-}Kit^+Sca1^-CD34^+CD16/32^+$), MEPs ($Lin^-c\text{-}Kit^+Sca1^-CD34^-CD16/32^-$), and CMPs ($Lin^-c\text{-}Kit^+Sca1^-CD34^+CD16/32^-$). Loss of HDAC6 did not affect the number and frequency of these LK subsets (Fig 1G–I). However, HDAC6 deficiency obviously decreased the frequency and number of the LSK subsets in the bone marrow, including MPPs ($Lin^-c\text{-}Kit^+Sca1^+Flk2^+CD34^+$), ST-HSCs ($Lin^-c\text{-}Kit^+Sca1^+Flk2^-CD34^+$), and LT-HSCs ($Lin^-c\text{-}Kit^+Sca1^+Flk2^-CD34^-$; Fig 1J–L), suggesting that HDAC6 specifically modulates the production of HSPCs.

We then proceeded to evaluate cell proliferation by measuring the proportion of cells incorporated with 5-ethynyl-2′-deoxyuridine (EdU), a pyrimidine analog of thymidine that can be incorporated into DNA in the S-phase of the cell cycle. HDAC6 deletion specifically decreased the proliferation of LK, LSK, MPP, and ST-HSC cells

Figure 1. Decreased proliferation of HSPCs in the bone marrow of *Hdac6* knockout mice.

A Schematic illustration of the strategy used for generating *Hdac6* knockout mice. Exons 10–13 of the mouse *Hdac6* gene were replaced by a vector containing neomycin (Neo) and zeocin (Zeo) cassettes.
B Genotypic identification of wild-type (WT) and *Hdac6* knockout (KO) mice.
C Cell number in the bone marrow of wild-type and *Hdac6* knockout mice (n = 12–13 mice per group).
D Flow cytometry profiles for the LK and LSK subsets in wild-type and *Hdac6* knockout mice.
E, F Frequency and number of the LK and LSK subsets in wild-type and *Hdac6* knockout mice (n = 12–13 mice per group).
G Flow cytometry profiles for the LK subset in wild-type and *Hdac6* knockout mice.
H, I Frequency and number of the LK subset in wild-type and *Hdac6* knockout mice (n = 12–13 mice per group).
J Flow cytometry profiles for the LSK subset in wild-type and *Hdac6* knockout mice.
K, L Frequency and number of the LSK subset in wild-type and *Hdac6* knockout mice (n = 12–13 mice per group).
M Flow cytometry profiles for the proportion of cycling HSPCs examined with EdU incorporation experiments.
N, O Frequency of the EdU-positive LK, LSK, MPP, ST-HSC, and LT-HSC subsets (n = 4–6 mice per group).
P Representative images of cell cycle for the LSK subsets in wild-type and *Hdac6* knockout mice.
Q The proportion of LSK subsets at different phases of the cell cycle in wild-type and *Hdac6* knockout mice (n = 3 mice per group).
R Representative images of colonies formed by bone marrow cells from wild-type and *Hdac6* knockout mice. Scale bar, 200 μm.
S Number of colonies formed by bone marrow cells from wild-type and *Hdac6* knockout mice (n = 10 mice per group).

Data information: All values are presented as mean ± SEM. *P < 0.05, **P < 0.01, ***P < 0.001, ****P < 0.0001, ns, not significant (Student's t-test). See also Fig EV1.
Source data are available online for this figure.

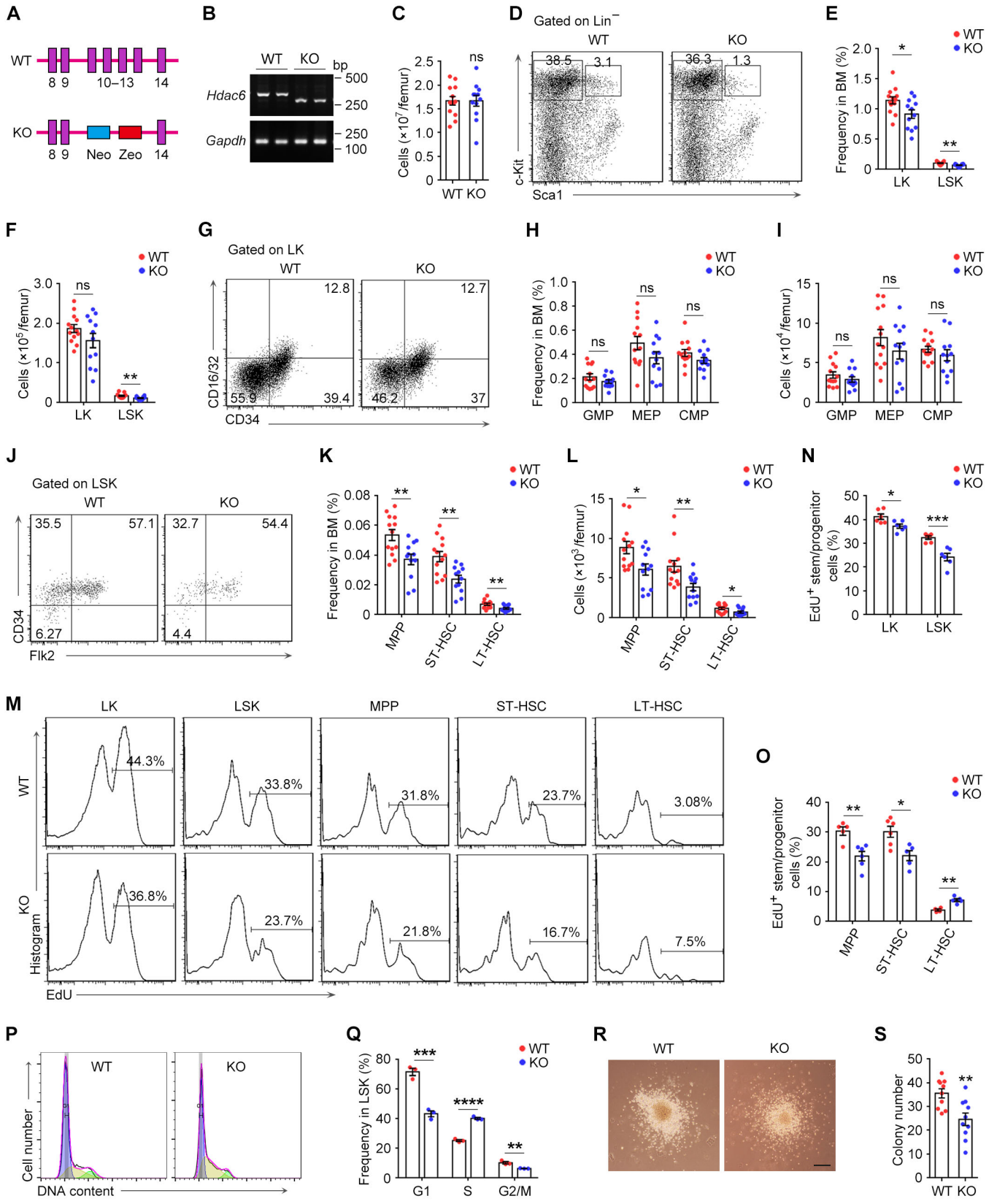
A
WT
8 9 10–13 14
KO
8 9 Neo Zeo 14
B
WT KO bp
Hdac6
Gapdh
500
250
250
100
C
Cells (×10^7/femur)
ns
WT KO
D
Gated on Lin−
WT KO
38.5 3.1
36.3 1.3
c-Kit
Sca1
E
Frequency in BM (%)
WT KO
LK LSK
F
Cells (×10^5/femur)
ns
**
LK LSK
G
Gated on LK
WT KO
12.8 12.7
55.9 39.4
46.2 37
CD16/32
CD34
H
Frequency in BM (%)
ns
GMP MEP CMP
I
Cells (×10^4/femur)
ns
GMP MEP CMP
J
Gated on LSK
WT KO
35.5 57.1
32.7 54.4
6.27 4.4
CD34
Flk2
K
Frequency in BM (%)
MPP ST-HSC LT-HSC
L
Cells (×10^3/femur)
MPP ST-HSC LT-HSC
N
EdU+ stem/progenitor cells (%)
LK LSK
M
LK LSK MPP ST-HSC LT-HSC
WT
44.3% 33.8% 31.8% 23.7% 3.08%
KO
36.8% 23.7% 21.8% 16.7% 7.5%
Histogram
EdU
O
EdU+ stem/progenitor cells (%)
MPP ST-HSC LT-HSC
P
WT KO
Cell number
DNA content
Q
Frequency in LSK (%)
G1 S G2/M
R
WT KO
S
Colony number
WT KO

Figure 1.

(Fig 1M–O). In addition, we confirmed that HDAC6 deletion did not affect the apoptosis of HSPCs (Fig EV1C).

In order to determine whether the decrease in the proliferation of bone marrow HSPCs in *Hdac6* knockout mice was due to cell cycle arrest or altered cell differentiation, we examined the cell cycle of LSK subsets in the bone marrow and the number and ratio of mature blood cells in the peripheral blood of wild-type and *Hdac6* knockout mice. We found that HDAC6 deficiency caused S-phase cell cycle arrest of LSK subsets (Fig 1P and Q), but did not affect the cell counts and ratio of mature blood cells in the peripheral blood (Fig EV1B and D). These results indicate that the reduced proliferation of bone marrow HSPCs in *Hdac6* knockout mice is due to cell cycle arrest.

To further analyze whether HDAC6 depletion decreases functional HSPCs *in vitro*, we performed granulocyte–monocyte colony formation assays. We found that the bone marrow cells from wild-type mice formed more colonies (35 colonies per 10,000 cells) than those from *Hdac6* knockout mice (22 colonies per 10,000 cells; Fig 1R and S), confirming the reduction in functional progenitor cells in the bone marrow of *Hdac6* knockout mice. Collectively, our results indicate that loss of HDAC6 inhibits the proliferation of HSPCs.

HDAC6 interacts with IDH1 both in cells and *in vitro*

To explore the molecular mechanisms underlying the regulation of HSPC proliferation by HDAC6, we immunoprecipitated HDAC6 from the whole lysate of mouse bone marrow cells and analyzed HDAC6-interacting proteins by mass spectrometry (Fig 2A). Kyoto Encyclopedia of Genes and Genomes (KEGG) pathway analysis of the proteins pulled down by HDAC6 identified the carbon metabolism pathway as one of the most enriched pathways, which includes IDH1 and several other proteins (Figs 2A, and EV2A and B). IDH1 is known to catalyze the oxidative decarboxylation of isocitrate to α-ketoglutarate (α-KG) and has been demonstrated to control the proliferation of HSPCs (Sasaki *et al*, 2012; Shi *et al*, 2015). Thus, we decided to focus on whether IDH1 is involved in the action of HDAC6 in regulating HSPC proliferation.

To confirm the interaction between HDAC6 and IDH1, HA-HDAC6 and GFP-IDH1 expression constructs were transfected into cells, and immunoprecipitation assays were performed. We found that GFP-IDH1 interacted with HA-HDAC6 in HEK293T cells (Fig 2B and C). Furthermore, endogenous HDAC6 could be immunoprecipitated by GFP-IDH1 (Fig 2D), and endogenous IDH1 could also be immunoprecipitated by HA-HDAC6 in HEK293T cells (Fig 2E). The specificity of the IDH1 antibody was verified by immunoblot analysis of the lysates of control and IDH1 knockdown cells (Fig EV2C). In addition, immunoprecipitation assays also revealed an interaction between endogenous HDAC6 and endogenous IDH1 in mouse bone marrow cells (Fig 2F). To analyze whether HDAC6 interacts with IDH1 directly, GST-IDH1 was overexpressed and purified from HEK293T cells, and HDAC6 was purified from Sf9 insect cells. By GST pulldown assays, we found that purified HDAC6 could interact with purified GST-IDH1, suggesting a direct interaction between these two proteins (Fig 2G).

To identify the structural domains mediating the interaction between HDAC6 and IDH1, we constructed a series of plasmids expressing different truncated forms of HDAC6 and IDH1 (Fig 2H and I). By immunoprecipitation assays, we found that a mutant of HDAC6 lacking the carboxyl terminus (1–840), a mutant harboring only the second deacetylase domain (416–840), and a mutant lacking the first deacetylase domain, Δ(84–412), could bind to IDH1, whereas a mutant of HDAC6 lacking the second deacetylase domain, Δ(416–840), and a mutant lacking both the second deacetylase domain and the carboxyl terminus (1–415) could not bind to IDH1 (Fig 2J). These results indicate that the second deacetylase domain is both required and sufficient for HDAC6 to interact with IDH1. Immunoprecipitation assays also revealed that the 101–415 and 206–310 fragments of IDH1 could bind to HDAC6, but the 1–93, 1–100, 101–205, and 311–415 mutants of IDH1 could not (Fig 2K), suggesting that the 206–310 fragment of IDH1 is both necessary and sufficient for its interaction with HDAC6.

HDAC6 deacetylates IDH1 at lysine 233 (K233)

The association between IDH1 and HDAC6 suggests that HDAC6 may deacetylate IDH1. To test this hypothesis, the acetylation of IDH1 was examined by immunoprecipitation with the acetyl-lysine antibody followed by immunoblotting with the IDH1 antibody, or by immunoprecipitation with the IDH1 antibody followed by immunoblotting with the acetyl-lysine antibody in bone marrow cells from wild-type and *Hdac6* knockout mice (Fig 3A and B). We found that the level of IDH1 acetylation increased significantly in *Hdac6* knockout bone marrow cells compared with the wild-type group. Two different HDAC6-specific siRNAs were then employed to deplete the expression of HDAC6 in HEK293T cells, and the acetylation of IDH1 was found to be significantly increased in HDAC6 knockdown cells (Fig 3C). Consistently, overexpression of HDAC6 decreased the acetylation of IDH1 in HEK293T cells (Fig 3D).

Figure 2. HDAC6 interacts with IDH1 both in cells and *in vitro*.

A Coomassie blue staining of proteins immunoprecipitated from the whole lysate of the mouse bone marrow cells, with the HDAC6 antibody or control IgG.
B, C Immunoprecipitation and immunoblotting showing the interaction of HA-HDAC6 with GFP-IDH1 in HEK293T cells.
D Immunoprecipitation and immunoblotting showing the interaction of GFP-IDH1 with endogenous HDAC6 in HEK293T cells.
E Immunoprecipitation and immunoblotting showing the interaction of HA-HDAC6 with endogenous IDH1 in HEK293T cells.
F Immunoprecipitation and immunoblotting showing the interaction between endogenous HDAC6 and endogenous IDH1 in bone marrow cells.
G GST pulldown and immunoblotting showing the interaction between purified GST-IDH1 and purified HDAC6.
H, I Schematic diagrams showing the structural domains of (H) HDAC6 and (I) IDH1 and various truncated mutants. DD, deacetylase domain.
J Immunoprecipitation and immunoblotting with various truncated mutants of HA-HDAC6 to identify the domains that mediate its interaction with GFP-IDH1.
K Immunoprecipitation and immunoblotting with various truncated mutants of GFP-IDH1 to identify the domains that mediate its interaction with HA-HDAC6. See also Fig EV2.

Source data are available online for this figure.

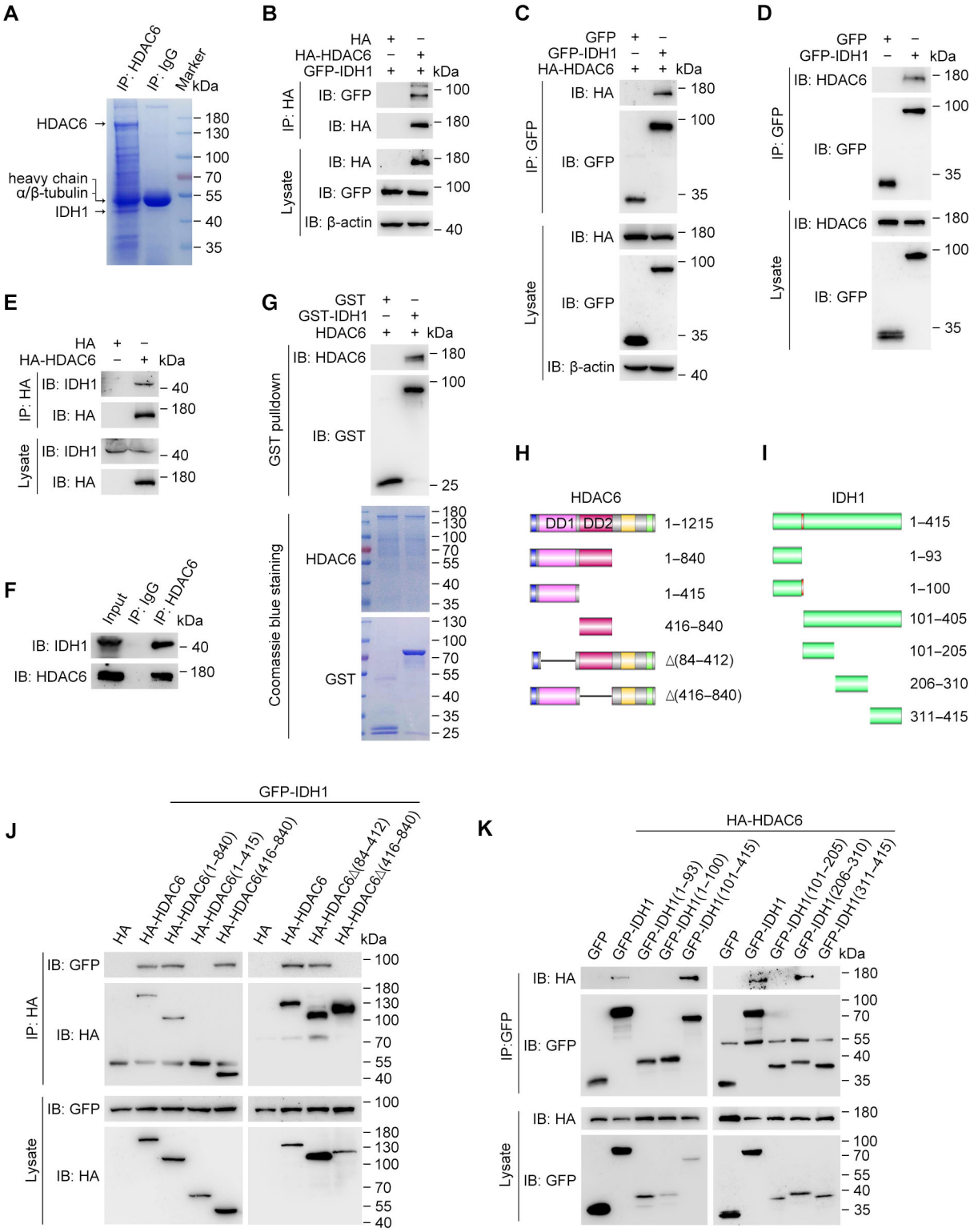

Figure 2.

To determine whether the reduced acetylation of IDH1 is dependent on the catalytic activity of HDAC6, we treated HEK293T cells with tubacin (Haggarty *et al*, 2003) and tubastatin A (Butler *et al*, 2010), two specific inhibitors of HDAC6, and trichostatin A (TSA; Yoshida *et al*, 1990), an inhibitor of class I, IIa, and IIb HDACs, including HDAC6. We found that all of these inhibitors

could increase the level of IDH1 acetylation. By contrast, sodium butyrate (NaB; Sealy & Chalkley, 1978; Kilgore *et al*, 2010), an inhibitor of class I HDACs, could not increase IDH1 acetylation (Fig 3E).

Furthermore, we performed *in vitro* deacetylation assays using GST-IDH1 isolated from HEK293T cells as the substrate. We found that the level of GST-IDH1 acetylation was significantly decreased upon incubation with HA-HDAC6 immunoprecipitated from HEK293T cells (Fig 3F). Collectively, these results suggest that HDAC6 is a deacetylase of IDH1.

We then sought to identify the acetylated lysine residue(s) in IDH1. The UniProt database predicted three lysine residues in IDH1 that might be acetylated, that is, K224, K233, and K321. As IDH1 is an evolutionarily conserved protein, we speculated that the acetylated lysine(s) might be conserved during evolution. Alignment of IDH1 sequences from four different species (human, rat, mouse, and zebrafish) revealed that the three predicted residues are indeed highly conserved (Fig EV2D). IDH1 is known as a homodimeric NAD phosphate-dependent enzyme (Geisbrecht & Gould, 1999; Xu *et al*, 2004). We analyzed the 3D structure of IDH1 and found that K224, K233, and K321 are all located on the surface of this protein (Fig 3G). These analyses suggest potential acetylation of these three residues.

To examine whether the three lysine residues of IDH1 could be deacetylated by HDAC6, each of these lysine residues was mutated to an arginine residue (K to R) to block acetylation. The HDAC6 inhibitor tubacin significantly increased the acetylation of wild-type IDH1 and the K224R and K321R mutants, but not the K233R mutant (Fig 3H and I). In addition, siRNA-mediated knockdown of HDAC6 expression revealed similar results (Fig 3J and K). Consistent with these findings, overexpression of HDAC6 remarkably reduced the acetylation of wild-type IDH1 and the K224R and K321R mutants, but did not obviously affect the acetylation of the K233R mutant (Fig 3L and M).

To confirm the deacetylation of K233 by HDAC6, we performed *in vitro* deacetylation assays using GST-IDH1 wild-type and K233R mutant proteins isolated from HEK293T cells. We found that the level of K233R acetylation was significantly lower than that of the wild-type protein (Fig 3N). Moreover, HA-HDAC6 could deacetylate GST-IDH1 wild type, but not the K233R mutant (Fig 3O and P). In summary, these findings strongly suggest that K233 is the primary lysine residue in IDH1 targeted for deacetylation by HDAC6.

HDAC6-mediated deacetylation decreases IDH1 activity and promotes the proliferation of HSPCs

We then asked whether HDAC6-mediated K233 deacetylation regulates IDH1 activity. IDH1 is known to catalyze the oxidative decarboxylation of isocitrate to produce α-KG and NADPH (Geisbrecht & Gould, 1999). To measure IDH1 activity, we sorted LSK cells from the bone marrow of wild-type and *Hdac6* knockout mice using flow cytometry. We found that IDH1 activity in *Hdac6* knockout LSK cells was significantly higher than that in wild-type LSK cells (Fig 4A). We also found that knockdown of HDAC6 efficiently increased the activity of IDH1 in HEK293T cells (Fig 4B). In addition, inhibition of HDAC6 activity with tubacin increased IDH1 activity and cellular α-KG level in a concentration-dependent manner (Fig 4C and D).

To examine the effect of HDAC6-mediated K233 deacetylation on IDH1 activity, we transfected HEK293T cells with plasmids expressing GFP-tagged IDH1 wild type, K233R (acetylation-deficient), or K233Q (acetylation-mimicking). The levels of these exogenously expressed GFP-tagged IDH1 proteins were markedly higher than endogenous IDH1 (Fig 4E). We compared the activities of these different IDH1 forms and found that the K233R mutant had a markedly lower activity than wild-type IDH1, whereas the K233Q mutant exhibited a higher activity than the wild type (Fig 4F). To verify whether HDAC6-mediated deacetylation reduces IDH1 activity, we transfected HDAC6-depleted HEK293T cells with plasmids expressing GFP-IDH1 wild type, K233R, or K233Q. We found that the K233R mutant, but not wild-type IDH1 or the K233Q mutant, largely blocked the promoting effect of HDAC6 depletion on IDH1 activity (Fig 4G and H). Next, we purified GST-tagged IDH1 wild type, K233R, and K233Q from HEK293T cells, and assessed their catalytic activities. We found that wild-type IDH1 possessed higher activity

Figure 3. HDAC6 deacetylates IDH1 at K233.

A Analysis of IDH1 acetylation via immunoprecipitation of the bone marrow cell lysate with the acetylated lysine (Ace-lysine) antibody, followed by immunoblotting with the IDH1 antibody.

B Analysis of IDH1 acetylation via immunoprecipitation of the bone marrow cell lysate with the IDH1 antibody, followed by immunoblotting with the Ace-lysine antibody.

C–E Analysis of GFP-IDH1 acetylation by immunoprecipitation with the GFP antibody followed by immunoblotting with the Ace-lysine antibody. HEK293T cells were treated with HDAC6 siRNAs (C), transfected with the HA-HDAC6 plasmid (D), or treated with tubacin, tubastatin A (TubA), trichostatin A (TSA), or sodium butyrate (NaB) (E).

F *In vitro* deacetylation assay indicating the deacetylation of GST-IDH1 by HA-HDAC6. The black arrowhead indicates HA-HDAC6, while the white arrowhead marks GST-IDH1.

G 3D structure of IDH1 showing the location of the three predicted acetylation sites.

H–M Immunoprecipitation and immunoblotting showing the level of IDH1 acetylation in HEK293T cells transfected with wild-type GFP-IDH1 or various mutants, and quantitative statistics was performed. These cells were treated with the HDAC6 inhibitor, tubacin (H, I), transfected with the HDAC6 siRNA (J, K), or transfected with the HA-HDAC6 plasmid (L, M). I, K, and M are the corresponding statistical results (n = 3 technical replicates).

N Immunoblotting showing the acetylation of GST-IDH1 and GST-IDH1 K233R proteins purified from HEK293T cells. The black arrowhead indicates GST-IDH1 and GST-IDH1 K233R.

O, P *In vitro* deacetylation analysis using GST-IDH1 and GST-IDH1 K233R proteins as substrates. The black arrowhead indicates HA-HDAC6, while the white arrowhead marks GST-IDH1 and GST-IDH1 K233R. (P) is the corresponding statistical result (n = 3 technical replicates).

Data information: All values are presented as mean ± SEM. *P < 0.05, **P < 0.01, ***P < 0.001, ****P < 0.0001, ns, not significant (Student's t-test). See also Figs EV2 and EV4.
Source data are available online for this figure.

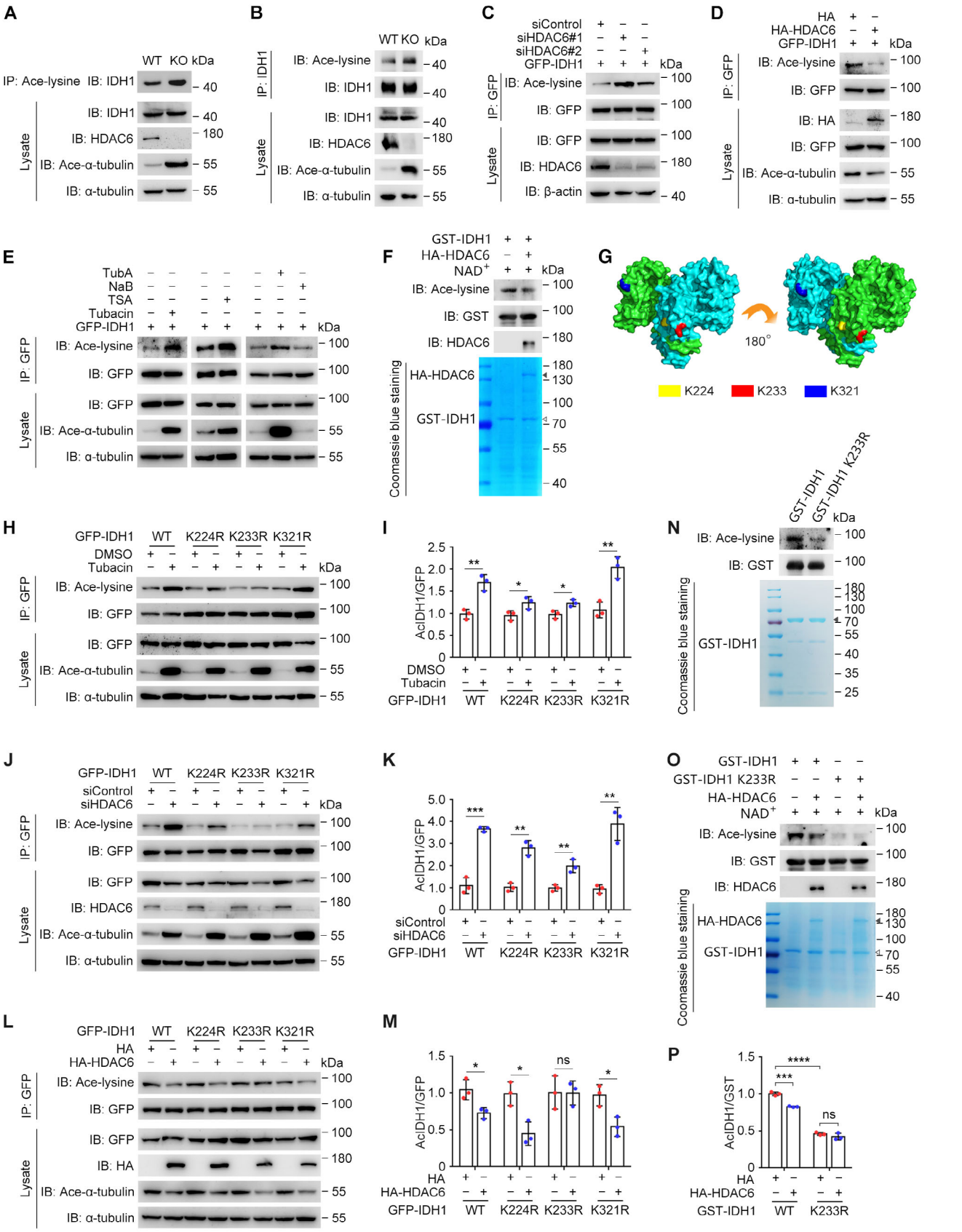
A
WT KO kDa
IP: Ace-lysine IB: IDH1
IB: IDH1
IB: HDAC6
IB: Ace-α-tubulin
IB: α-tubulin
Lysate
B
IP: IDH1
IB: Ace-lysine
IB: IDH1
IB: HDAC6
IB: Ace-α-tubulin
IB: α-tubulin
C
siControl
siHDAC6#1
siHDAC6#2
GFP-IDH1
IP: GFP
IB: Ace-lysine
IB: GFP
IB: HDAC6
IB: β-actin
D
HA
HA-HDAC6
GFP-IDH1
IP: GFP
IB: Ace-lysine
IB: GFP
IB: HA
IB: Ace-α-tubulin
E
TubA
NaB
TSA
Tubacin
F
GST-IDH1
HA-HDAC6
NAD+
IB: Ace-lysine
IB: GST
IB: HDAC6
Coomassie blue staining
G
180°
K224
K233
K321
H
GFP-IDH1 WT K224R K233R K321R
DMSO
Tubacin
I
AcIDH1/GFP
N
GST-IDH1
GST-IDH1 K233R
O
GST-IDH1
GST-IDH1 K233R
J
siControl
siHDAC6
K
L
M
P
AcIDH1/GST

Figure 3.

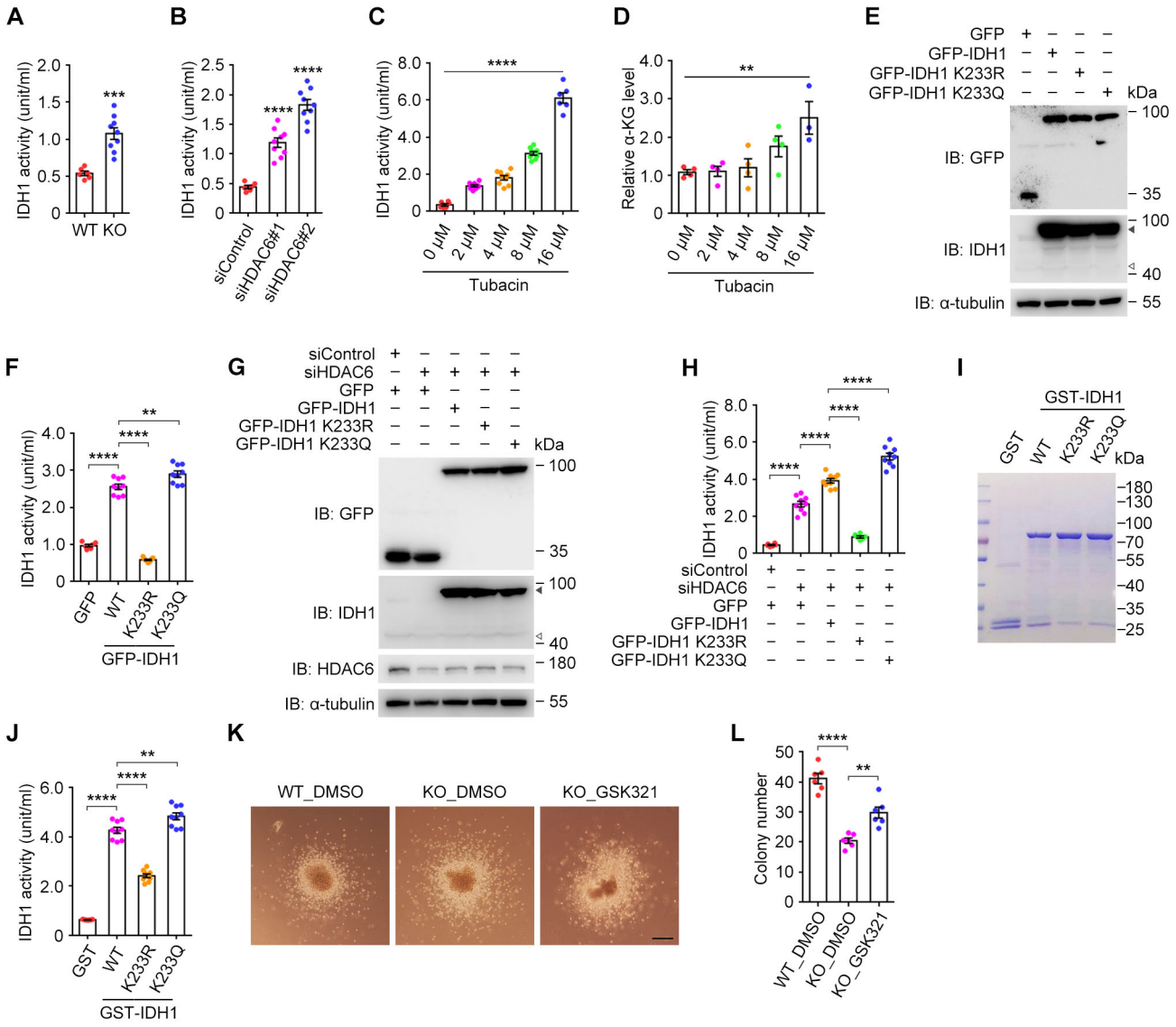

Figure 4. HDAC6-mediated deacetylation inhibits IDH1 activity and promotes the proliferation of HSPCs.

A Analysis of IDH1 activity in wild-type and *Hdac6* knockout bone marrow cells (n = 6–9 tests from three independent experiments).

B Analysis of IDH1 activity in HEK293T cells transfected with control or HDAC6 siRNAs (n = 6–9 tests from three independent experiments).

C Analysis of IDH1 activity in HEK293T cells treated with the indicated concentration of tubacin (n = 6–9 tests from three independent experiments).

D Analysis of the α-KG level in HEK293T cells treated with the indicated concentration of tubacin (n = 4 independent experiments).

E, F Immunoblotting (E) and IDH1 activity analysis (F, n = 6–9 tests from three independent experiments) in HEK293T cells transfected with plasmids expressing GFP, GFP-IDH1, GFP-IDH1 K233R, or GFP-IDH1 K233Q. In panel (E), the black arrowhead indicates exogenous IDH1, while the white arrowhead marks endogenous IDH1.

G, H Immunoblotting (G) and IDH1 activity analysis (H, n = 6–9 tests from three independent experiments) in HEK293T cells transfected with control or HDAC6 siRNAs, and plasmids expressing GFP, GFP-IDH1, GFP-IDH1 K233R, or GFP-IDH1 K233Q. In panel (G), the black arrowhead indicates exogenous IDH1, while the white arrowhead marks endogenous IDH1.

I, J Coomassie blue staining (I) and IDH1 activity analysis (J, n = 9 tests from three independent experiments) of the purified proteins.

K Representative images of the colony formation assay. Scale bar, 200 μm.

L Number of colonies formed by wild-type and *Hdac6* knockout mice bone marrow cells treated or untreated with 10 μM GSK321 (n = 6 mice per group).

Data information: All values are presented as mean ± SEM. $^{**}P < 0.01$, $^{***}P < 0.001$, $^{****}P < 0.0001$ (Student's t-test for panel A, and ANOVA test for panels B, C, D, F, H, J, and L).
Source data are available online for this figure.

than the K233R mutant, but lower activity than the K233Q mutant (Fig 4I and J). Taken together, these findings indicate that HDAC6-mediated K233 deacetylation reduces IDH1 activity.

To further investigate whether HDAC6 promotes the production of HSPCs through regulating the enzymatic activity IDH1, we performed granulocyte–monocyte colony formation assays using

Hdac6 knockout bone marrow cells treated with GSK321, a chemical compound that could inhibit mutant IDH1 at low concentrations and wild-type IDH1 at high concentrations (Okoye-Okafor *et al*, 2015; Jiang *et al*, 2016; Xu *et al*, 2020; Dai *et al*, 2022). We found that *Hdac6* knockout bone marrow cells formed fewer colonies than wild-type cells, and inhibition of IDH1 activity by the addition of GSK321 (10 μM) restored the colony forming ability of *Hdac6* knockout bone marrow cells (Fig 4K and L). These results indicate that HDAC6 regulates the proliferation of HSPCs by affecting the catalytic activity of IDH1.

HDAC6-mediated IDH1 deacetylation promotes cell proliferation and inhibits the hydroxymethylation of TET2 target genes

The production of α-KG by IDH1 is essential for the activity of the TET family of oxidases, which catalyze the hydroxylation of 5-methylcytosine (5mC) to 5hmC, leading to DNA demethylation and gene expression regulation (Tahiliani *et al*, 2009). It has been reported that *Tet2* knockout HSCs exhibit enhanced self-renewal capacity (Ko *et al*, 2011; Moran-Crusio *et al*, 2011; Quivoron *et al*, 2011). IDH1/2 mutation can regulate the level of 5hmC by modulating TET2 activity, thereby influencing the number of HSPCs (Figueroa *et al*, 2010). Based on our finding that HDAC6-mediated deacetylation decreased IDH1 activity, we hypothesized that altered 5hmC levels on target genes could be a mechanism underlying HDAC6-promoted HSPC proliferation. To test this hypothesis, we sorted LSK cells from mouse bone marrow using flow cytometry (Fig 5A). Global genome methylation and hydroxymethylation sequencing were performed using oxidative bisulfite sequencing (oxBS-Seq). Our results revealed that the mean DNA methylation rates in wild-type and *Hdac6* knockout LSK cells were 82.52 and 81.39%, respectively. Additionally, the mean hydroxymethylation rates were 5.68 and 5.63%, respectively. According to the read count, the genomic distribution of 5hmC in wild-type and *Hdac6* knockout LSK cells presents no obvious difference (Fig 5B).

In order to validate whether the hyperacetylation of IDH1 resulting from *Hdac6* knockout leads to elevated hydroxymethylation of TET2 target genes and consequently inhibits proliferation, we constructed a TET2 target gene dataset based on TET2 ChIP-seq results (Rasmussen *et al*, 2019). We then analyzed this dataset along with the significantly upregulated hydroxymethylation genes, identifying 2,919 overlapping genes (Fig 5C), including several genes that negatively regulate cell proliferation (Fig 5D). Cell proliferation-related TET2 target genes, including *Ppp2r5b*, *Birc5*, *Nsun2*, *Pinx1*, *Rrp8*, and *Col18a1*, were hyper-hydroxymethylated in *Hdac6* knockout LSK cells (Fig 5E), while TET2-independent genes, including *Cep19*, *Dvl1*, and *Etv3l*, showed no difference in their hydroxymethylation levels (Fig 5F). These findings suggest that *Hdac6* knockout promotes the hydroxymethylation of TET2 target genes and further regulates the proliferation of HSPCs.

α-KG has been shown to function as a cofactor for JmjC domain-containing histone demethylases (Tsukada *et al*, 2006), in addition to its role in 5hmC-mediated DNA demethylation. Therefore, we speculated that HDAC6-mediated IDH1 deacetylation might also influence the level of histone methylation. To test this possibility, we analyzed the monomethylation of histone H3K4 and the trimethylation of H3K4, H3K9, H3K27, and H3K36 by immunoblotting with specific antibodies. We found that these histone methylations were not affected by inhibition of HDAC6 activity, depletion of HDAC6 expression, or mutation of the K233 residue in IDH1 (Fig EV3A–D). These data suggest that HDAC6-mediated IDH1 deacetylation specifically decreases the 5hmC level of TET2 target genes.

Hdac6 knockout alters the expression of TET2 target genes involved in the proliferation of HSPCs

The level of 5hmC plays a critical role in the regulation of gene expression and thereby is involved in a variety of biological processes (Shi *et al*, 2017). The relationship between the 5hmC level and gene expression patterns is complicated and cell type dependent (Shi *et al*, 2017). To further explore the mechanism by which elevated hydroxymethylation of TET2 target genes inhibits the expansion of LSK cells from *Hdac6* knockout bone marrow cells, we isolated LSK cells from the bone marrow of wild-type and *Hdac6* knockout mice by flow cytometry, and analyzed the transcriptome by RNA sequencing.

Bioinformatics analyses revealed a total of 271 significantly differentially expressed genes (DEGs) between wild-type and *Hdac6* knockout LSK cells with a fold change > 2 and a significance of *P*-value < 0.05 (Fig 6A). Among these DEGs, 109 genes were downregulated and 162 genes were upregulated in *Hdac6* knockout LSK cells (Fig 6B). Subsequently, we performed gene ontology (GO) enrichment analysis to explore the pathways associated with these DEGs. Our analysis demonstrated that loss of HDAC6 led to a significant upregulation of genes that negatively regulate the cell cycle (Fig 6C and D). By overlapping the TET2 target gene dataset, upregulated expression gene dataset, and upregulated hydroxymethylation gene dataset, we identified 62 overlapping genes (Fig 6E), including those involved in the negative regulation of the cell cycle. Quantitative PCR (qPCR) further confirmed that the mRNA levels of *Pinx1*, *Col18a1*, and *Ppp2r5b* were significantly increased in HDAC6 knockdown HEK293T cells (Fig 6F–H), and inhibition of IDH1 activity by the addition of GSK321 (10 μM) could suppress the upregulation of these genes (Fig 6I–K). *Pinx1* has been shown to inhibit the proliferation of bladder urothelial carcinoma cells and non-small cell lung cancer cells (Liu *et al*, 2013; Tian *et al*, 2017). *Col18a1* can suppress endothelial cell proliferation (O'Reilly *et al*, 1997; Kim *et al*, 2002), and *Ppp2r5b* can repress the proliferation of neuronal cells (Van Kanegan & Strack, 2009). These results support our finding that HDAC6-mediated IDH1 deacetylation promotes the proliferation of HSPCs by modulating the expression of TET2 target genes related to HSPC proliferation.

Discussion

The present study identifies an important function for HDAC6 in regulating the homeostasis of HSPCs (Fig 7). In particular, our data demonstrate that HDAC6 plays a critical role in maintaining the number and frequency of LSKs in the bone marrow. Mechanistically, our data reveal that HDAC6 interacts with IDH1 and deacetylates IDH1 at K233. Loss of HDAC6 increases the acetylation and enzymatic activity of IDH1, and subsequently increases the 5hmC level of TET2 target genes, thereby influencing gene expression to alter the proliferation of HSPCs (Fig 7).

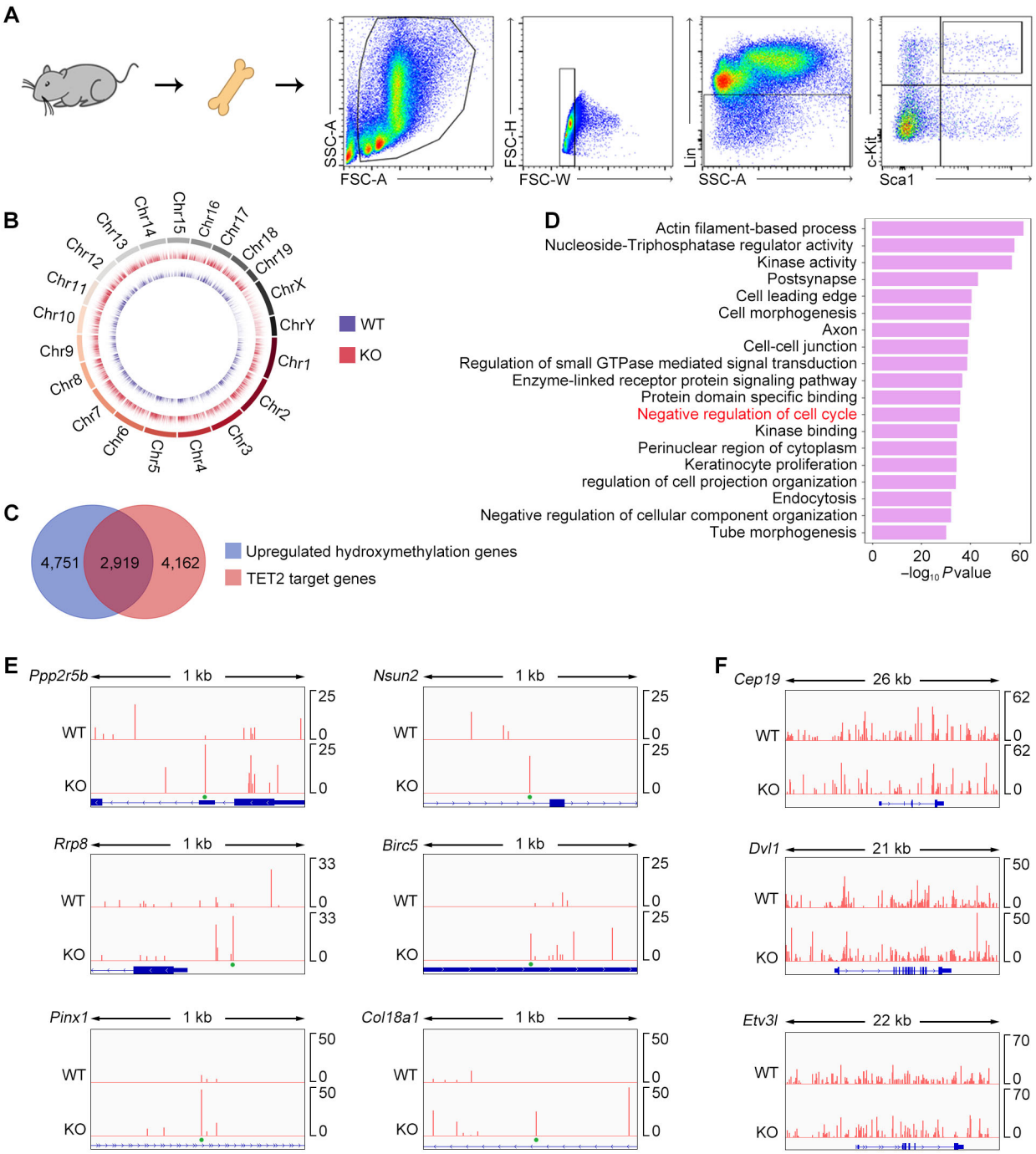

Figure 5. HDAC6-mediated IDH1 deacetylation promotes cell proliferation and inhibits the hydroxymethylation of TET2 target genes.

A Schematic illustration of the experimental setup used to acquire wild-type and *Hdac6* knockout LSK cells. Whole mouse bone marrow cells were taken, and after lysing the red blood cells, corresponding antibodies were labeled. $Lin^{-}c\text{-}Kit^{+}Sca1^{+}$ cells were flow cytometrically isolated for sequencing.

B Genome-wide distribution of hydroxymethylation in wild-type and *Hdac6* knockout LSK cells.

C Overlapping analysis of 7,670 upregulated hydroxymethylation genes (methdiff > 0.1, *P*-value < 0.05) and 7,081 TET2 targeted genes resulting in a total of 2,919 candidate genes.

D GO enrichment results of 2,919 overlapping genes.

E IGV screenshots showing elevated hydroxymethylation of multiple candidate genes associated with negative regulation of the cell cycle.

F IGV screenshots of TET2-independent genes showing no significant changes in hydroxymethylation. See also Fig EV3.

Source data are available online for this figure.

HSPCs maintain the stem cell pool through self-renewal, differentiation, and programmed death to meet the body's demand for various blood cells. A number of factors are known to control HSPC homeostasis, such as Wnt and Notch signaling molecules, miRNAs, inflammatory factors, epigenetic factors, and cell cycle regulators (Walker *et al*, 1999; Reya *et al*, 2003; Jiang *et al*, 2019; Sezaki *et al*, 2020; Chen *et al*, 2022; Crisafulli & Ficara, 2022). For example, high level of Wnt signaling promotes HSPC proliferation and inhibits cell differentiation (Reya *et al*, 2003). Inhibition of miR-99 induces cell differentiation and proliferation, thereby causing the exhaustion of the HSPC pool (Khalaj *et al*, 2017). IFN-α stimulates the quiescence of HSPCs and hence reduces the HSPC pool (Essers *et al*, 2009). Depletion of lysine-specific demethylase 1 inhibits HSPC self-renewal and differentiation, resulting in whole-blood cytopenia (Kerenyi *et al*, 2013). Loss of cyclin A inhibits the proliferation of HSPCs, resulting in severe anemia (Kalaszczynska

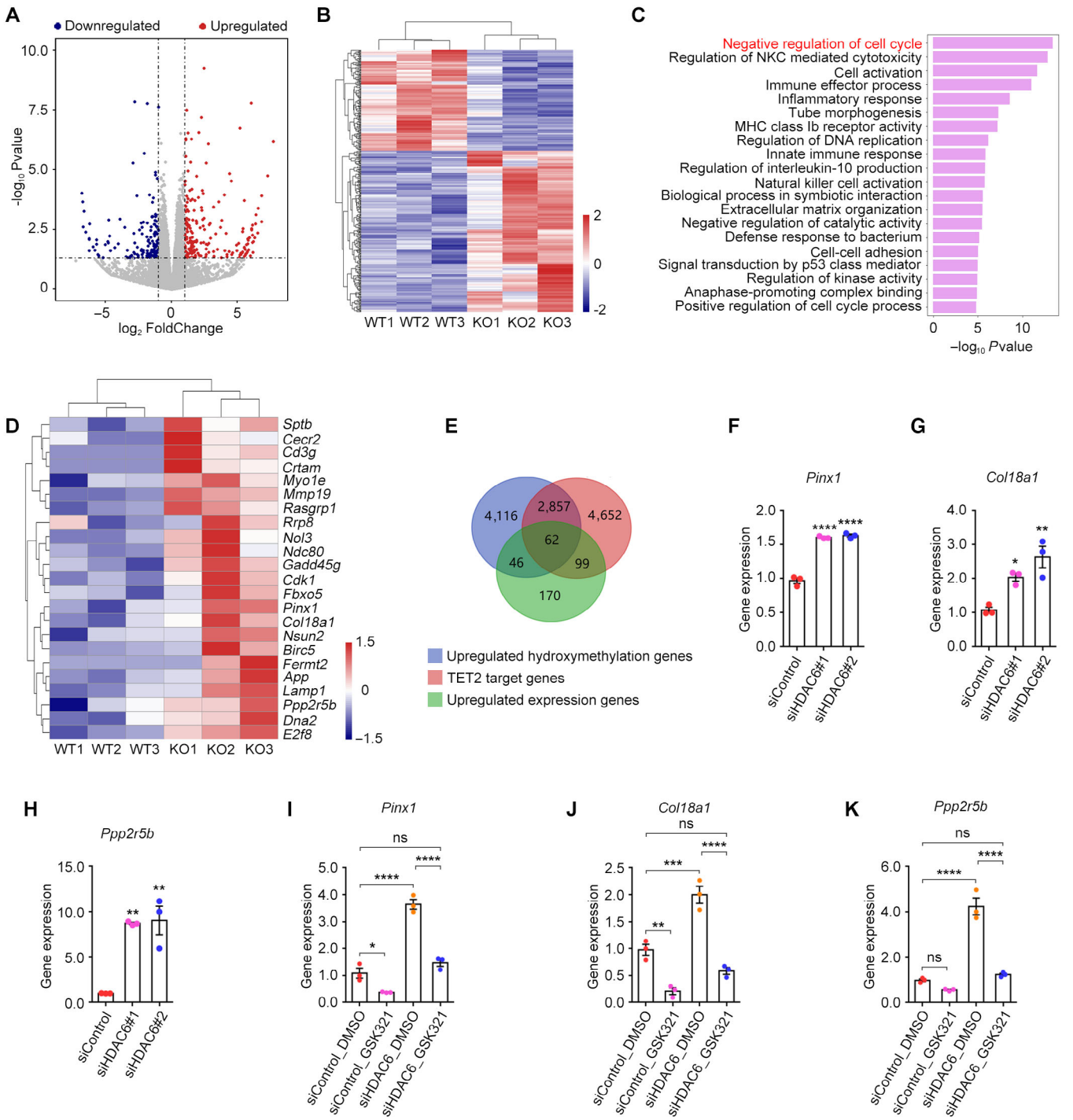

Figure 6.

Figure 6. *Hdac6* knockout alters the expression of TET2 target genes involved in the proliferation of HSPCs.

A Volcano plot showing the significant upregulation of 162 genes and significant downregulation of 109 genes by the loss of HDAC6 (Foldchange > 2, *P*-value < 0.05).
B Heatmaps showing differentially expressed genes (Foldchange > 2, *P*-value < 0.05).
C GO enrichment analysis of 377 upregulated genes by the loss of HDAC6 (FoldChange > 1.5, *P*-value < 0.05).
D Heatmaps based on the GO enrichment analysis showing genes that negatively regulate the cell cycle.
E Intersection analysis of 377 upregulated genes, 7,670 significantly upregulated hydroxymethylation genes, and 7,081 TET2-targeted genes.
F–H qPCR showing that knockdown of HDAC6 significantly upregulates the expression of TET2 target genes with hyper-hydroxymethylation.
I–K qPCR showing that treatment with 10 μM GSK321 inhibits the upregulation of the indicated genes in HDAC6 knockdown HEK293T cells.

Data information: All values are presented as mean ± SEM. **P* < 0.05, ***P* < 0.01, ****P* < 0.001, *****P* < 0.0001, ns, not significant (ANOVA test).
Source data are available online for this figure.

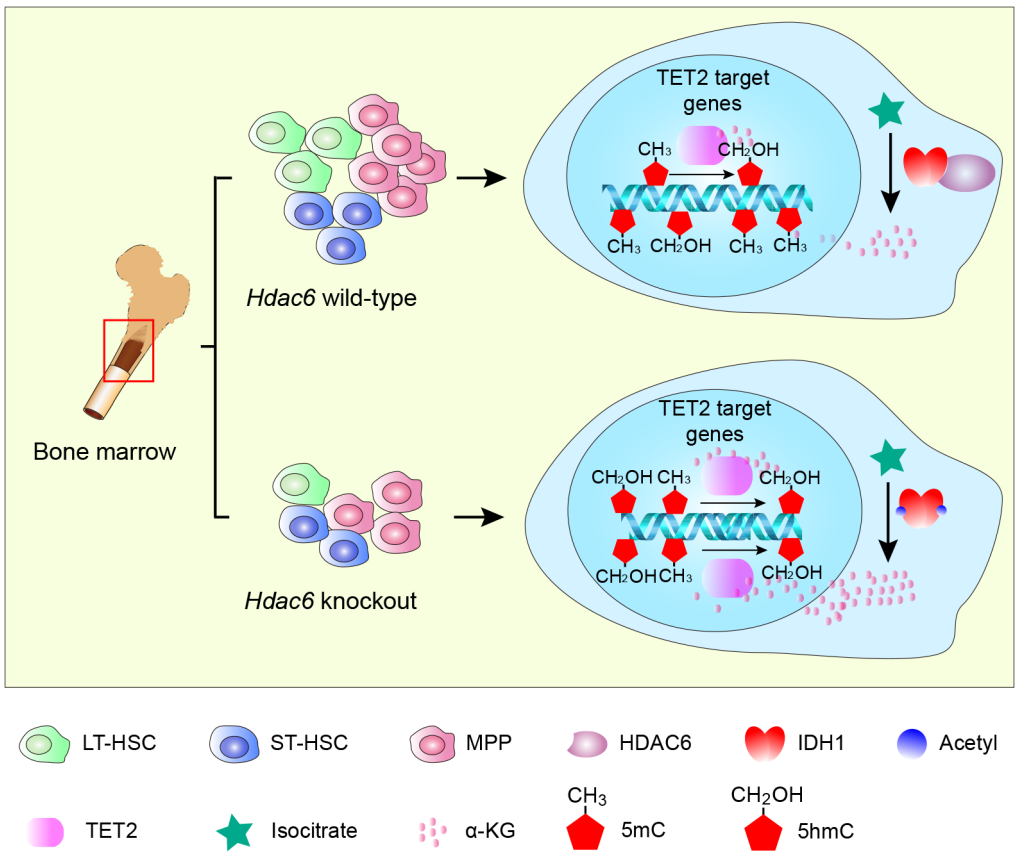

Figure 7. Schematic diagram showing the function of HDAC6-mediated IDH1 deacetylation in regulating the proliferation of HSPCs.
In mouse bone marrow HSPCs, HDAC6 interacts with IDH1 and deacetylates IDH1 at K233. The deacetylation of IDH1 inhibits its enzymatic activity and thereby decreases the 5hmC level of TET2 target genes to maintain HSPC homeostasis. *Hdac6* deficiency increases the acetylation and activity of IDH1, thereby elevating the 5hmC level of TET2 target genes, and changing gene expression patterns to inhibit the proliferation of HSPCs.

et al, 2009). Depletion of Cyclin D also leads to reduced proliferation of HSPCs in mouse fetal liver and the inability to reconstruct the cell lineages in irradiated mice (Kozar *et al*, 2004).

In this study, our data demonstrate that HDAC6 regulates the proliferation of HSPCs, but not their apoptosis or differentiation (Figs 1M–O, and EV1C and D). In addition, *Hdac6* knockout mice survive well and do not show obvious phenotypes despite the abnormal HSPCs. These findings suggest that the reduced HSPCs in mice due to HDAC6 deficiency may still meet normal physiological needs in the absence of severe inflammation. It is also tempting to speculate that impaired hematopoiesis may occur in *Hdac6* knockout mice in response to certain stimuli. Interestingly, our data also reveal a significant increase in the proliferation of LT-HSCs in *Hdac6* knockout mice. This is probably due to a feedback regulation caused by the reduced number of HSPCs. Further studies are warranted for in-depth investigation of the mechanisms of how HDAC6 regulates hematopoiesis under pathological conditions.

Members of the HDAC family have been implicated previously in the regulation of HSPC homeostasis. For example, reduction in HDAC3 in the cord blood cells maintains the stemness of HSCs and expands the HSCs pool, whereas reduction in HDAC1, HDAC2, and HDAC8 inhibits the differentiation of HSCs into the monocyte lineage (Elizalde *et al*, 2012). HDAC1 and HDAC3 inhibit the transcriptional activity of RUNX1, thereby inhibiting the proliferation of HSCs (Guo & Friedman, 2011). HDAC3 and HDAC5, but not HDAC1, can interact with GATA2 and inhibit its transcriptional activity, thus playing a role in HSC proliferation (Ozawa *et al*, 2001). HDAC3 is highly expressed in HSPCs and regulates the proliferation of HSPCs (Dhoke *et al*, 2016). While most other HDACs function at the transcriptional level through deacetylating histones in the nucleus, HDAC6 is mainly localized and functions in the cytoplasm (Verdel *et al*, 2000). Our results demonstrate that HDAC6 deacetylates IDH1 and regulates IDH1 activity, thereby playing an important role in the proliferation of HSPCs. IDH1-catalyzed production of α-KG is an important cofactor for dioxygenases, such as the TET family members (Tahiliani *et al*, 2009), which catalyze the formation of 5hmC from 5mC in genomic DNA, further regulating gene expression (Shi *et al*, 2017; Wu & Zhang, 2017; Wu *et al*, 2018; Lio *et al*, 2019). Although HDAC6 does not directly catalyze the deacetylation of histones to mediate transcriptional regulation, our findings reveal an indirect function of HDAC6 in epigenetic regulation through deacetylating IDH1.

At present, most of the studies on IDH1 focus on the arginine 132 residue (R132), which is essential for the catalytic activity of IDH1. R132 mutation changes the catalytic product of IDH1 to produce (R)-2-hydroxyglutarate (α-HG), which inhibits the activity of α-KG-dependent dioxygenases, altering the levels of DNA/histone methylation (Dang *et al*, 2009; Figueroa *et al*, 2010; Gross *et al*, 2010; Xu *et al*, 2011). Mutations in R132 have been shown to cause severe hematopoietic diseases, including acute myeloid leukemia and myelodysplastic syndromes (Gross *et al*, 2010; Thol *et al*, 2010). In this study, we have discovered an important role for K233 acetylation in regulating IDH1 activity. Our results also suggest that K233 exists in a region that mediates the interaction between two IDH1 monomers (Fig EV4A–C), and the deacetylation of IDH1 by HDAC6 inhibits the formation of IDH1 homodimers (Fig EV4D and E), leading to decreased catalytic activity.

In summary, the present study uncovers the critical role of the HDAC6-IDH1 axis in regulating the homeostasis of HSPCs. Our findings may have important implications in the treatment of hematological diseases.

Materials and Methods

Mice

C57BL/6 *Hdac6* knockout mice were kindly provided by Professor Tso-pang Yao from Duke University. Wild-type mice and *Hdac6* knockout mice were bred in the specific pathogen free (SPF) barrier of the Experimental Animal Center at Nankai University. All mouse experiments were approved by and performed in accordance with the guidelines of the Animal Care and Use Committee of Nankai University. Randomization and blinding were not employed for animal experiments.

Antibodies

The following antibodies were used: anti-GFP (11814460001, Roche, Basel, Switzerland), anti-HA (H3663, Sigma-Aldrich, Missouri, USA), anti-GST (G7781, Sigma-Aldrich), anti-Ace-α-tubulin (T6793, Sigma-Aldrich), anti-α-tubulin (T6199, Sigma-Aldrich), anti-acetylated lysine (PTM-101, PTM, Hangzhou, China), anti-β-actin (AC026, ABclonal, Wuhan, China), anti-HDAC6 (07-732, Millipore, Massachusetts, USA), anti-IDH1 (12332-1-AP, Proteintech, Chicago, USA), anti-histone H3 (9715, Cell Signaling Technology, Massachusetts, USA), anti-H3K4me1 (ab8895, Abcam, Cambridge, UK), anti-H3K4me3 (ab8580, Abcam), anti-H3K9me3 (ab8898, Abcam), anti-H3K27me3 (ab6002, Abcam), and anti-H3K36me3 (4909, Cell Signaling Technology). Anti-GFP agarose (D153-8) was purchased from Medical & Biological Laboratories (Tokyo, Japan). Anti-HA agarose (M20031) was purchased from Abmart Shanghai Ltd. (Shanghai, China). Mouse anti-goat IgG-HRP (sc-2354) and rabbit anti-goat IgG-HRP (sc-2768) were purchased from Santa Cruz Biotechnology (Oregon, USA). Fluorescein (FITC)-conjugated goat anti-mouse IgG (H + L) (115-095-003), rhodamine (TRITC)-conjugated goat anti-mouse IgG (H + L) (115-025-003), FITC-conjugated goat anti-rabbit IgG (H + L) (111-095-003), and TRITC-conjugated goat anti-rabbit IgG (H + L) (111-025-003) were purchased from Jackson ImmunoResearch Laboratories (Pennsylvania, USA). Mouse CD117 (c-Kit) MicroBeads (130-091-224) and LS columns (130-122-729) were purchased from Miltenyi Biotec (Bergisch Gladbach, Germany), PE/Cyanine7 streptavidin (405206), APC/Cyanine 7 anti-mouse Ly-6A/E (Sca1) antibody (108125), PE anti-mouse Ly-6A/E (Sca1) antibody (160905), APC anti-mouse CD117 (c-Kit) antibody (161505), PE anti-mouse CD135 (FLT3/FLK2) antibody (135305), PerCP/Cyanine 5.5 anti-mouse CD16/32 antibody (101323), PerCP anti-mouse/human CD45R/B220 antibody (103233), PerCP anti-mouse/human CD11b antibody (101229), PerCP anti-mouse TER-119/erythroid cells antibody (116225), and PerCP anti-mouse CD3ε antibody (100325) were all purchased from BioLegend (California, USA). FITC-conjugated CD34 monoclonal antibody (11-0349-42) was purchased from Thermo Fisher Scientific Inc. (Massachusetts, USA).

Chemicals

DAPI (D5942), TSA (V900931), and NaB (B5887) were purchased from Merck KGaA (Darmstadt, Germany). GSK321 (HY-18948) was purchased from MedChemExpress LLC (New Jersey, USA). Hoechst 33342 was purchased from Guangzhou RiboBio (Guangzhou, China). Glutathione Sepharose 4B was purchased from GE Healthcare (17-0756-01, Chicago, USA). Pan anti-acetyl-lysine antibody-conjugated agarose (PTM-103) was purchased from PTM Biolabs. Protein A/G agarose (20422) was purchased from Thermo Fisher Technology. Lineage Cell Detection Cocktail-Biotin (130-092-613) was purchased from Miltenyi Biotec.

Plasmids, siRNAs, and primers

Plasmids expressing HA-HDAC6 were described previously (Huo *et al*, 2011). All siRNAs were purchased from Guangzhou RiboBio (Guangzhou, China). The following siRNAs were used in this study: control siRNA: CGUACGCGGAAUACUUCGA; human HDAC6 siRNA#1: GCAGUUAAAUGAAUUCCAU; human HDAC6 siRNA#2:

GGAGUUAACUGGCAGGCAU; human IDH1 siRNA#1: GCATAA TGTTGGCGTCAAA; human IDH1 siRNA#2: GTCCCAGTTTGAA GCTCAA; and human IDH1 siRNA#3: GGCCCAAGCTATGAAATCA. The primer sequences for mouse genotype identification are as follows: *Hdac6*-Int-9: CTGGTTCGTCTGAAGACA, *Hdac6*-Exo-10: GTGG ACCAGTTAGAAGCC, *Hdac6*-Zeo-1: CCATGACCGAGATCGGCGAG CA, *Hdac6*-Zeo-3: CGTGAATTCCGATCATATTCAAT; *Gapdh*-F: CG CCTGGAGAAACCTGTATGTATG, *Gapdh*-R: GAAGAGTGGGAGTTG CTGTTGAAG. The primer sequences for qPCR are as follows: *Pinx1*-F: CCAGAGGAGAACGAAACCACG, *Pinx1*-R: ACCTGCGTCTCAGAAA TGTCA, *Col18a1*-F: TGGTCTACGTGTCGGAGCA, *Col18a1*-R: GCCTC GTTCGCCCTTAGAG, *Ppp2r5b*-F: AGCCCGTCTACCCAGACATC, *Ppp2r5b*-R: CCAAGAAACGCAGGAAAAACTC.

Cell culture and transfection

HEK293T cells were purchased from the American Type Culture Collection (ATCC, Manassas, VA, USA). Cells were cultured in Dulbecco's modified Eagle's medium (DMEM) supplemented with 10% fetal bovine serum (FBS, C04001-500, VivaCell Biosciences, Shanghai, China) at 37°C in a humidified atmosphere with 5% CO_2. Plasmids were transfected into cells using polyethylenimine (PEI, 23966-1, Polysciences, Pennsylvania, USA) and siRNAs were transfected using the Lipofectamine RNAiMAX transfection reagent (13778030, Invitrogen, California, USA).

Flow cytometry and cell sorting

Bone marrow cells from femurs and tibias were flushed in PBS with 2% FBS. Red blood cells were lysed using ACK buffer (A1049201, Gibco, California, USA). Then, a total of 2–5 × 10^6 bone marrow cells were incubated with Lineage Cell Detection Cocktail-Biotin in PBS. After washed, the cells were labeled with corresponding antibodies. PE/Cyanine 7 streptavidin was used to label biotin. APC/Cyanine 7 anti-mouse Ly-6A/E (Sca1) and APC anti-mouse CD117 (c-Kit) were used to label HSPCs. FITC anti-mouse CD34 and PE anti-mouse CD135 (FLT3/FLK2) were used to label the LSK subset. FITC anti-mouse CD34 and PerCP/Cyanine 5.5 anti-mouse CD16/32 were used to label the LK subset. Samples were incubated with antibodies at 4°C for 90 min, washed, and then subjected to flow cytometry. For cell sorting, bone marrow cells were stained with lineage marker antibodies (PerCP anti-mouse/human CD45R/B220, PerCP anti-mouse/human CD11b, PerCP anti-mouse TER-119/erythroid cells, and PerCP anti-mouse CD3ε) and HSPCs marker antibodies (PE anti-mouse Sca1 and APC anti-mouse CD117 (c-Kit)) at 4°C for 30 min, and then the LSK cells ($Lin^-c\text{-}Kit^+Sca1^+$) were sorted on BD FACSAria Fusion.

EdU incorporation assay

The click-iT Plus EdU Alexa Fluor 647 Flow Cytometry Assay Kit (C10634, Invitrogen) was used according to the manufacturer's instructions. Briefly, EdU (0.5 mg/mouse) was intraperitoneally injected into mice. Twenty hours later, whole bone marrow cells were obtained, red blood cells were lysed, and the remaining cells were labeled with corresponding antibodies. Then, the cells were incubated with Click-iTTM fixative and Click-iTTM saponin-based permeabilization for 15 min successively and resuspended in Click-iTTM Plus reaction cocktail for 30 min at room temperature in the dark. After washed with Click-iTTM saponin-based permeabilization, the cells were resuspended in 500 μl Click-iTTM saponin-based permeabilization and subjected to flow cytometry.

Cell cycle analysis and apoptosis assay

To analyze the cell cycle, bone marrow cells were obtained from mice, and c-Kit microbeads were used to enrich the c-Kit positive cell population. Cells were then labeled with corresponding antibodies and incubated with Hoechst 33342 at 37°C for 30 min in the dark. Cells were resuspended in PBS and then subjected to flow cytometry. To analyze apoptosis, the c-Kit positive population was labeled with DAPI and then subjected to flow cytometry.

Colony formation assay

1 × 10^4 bone marrow cells in 1 ml medium (MethoCult™ GF M3434, StemCell) were added to a well of a 24-well plate, and cultured for a week. The number of cell colonies was counted under a microscope.

GST pulldown assay

For each GST pulldown assay, 5 μg of GST-IDH1 or GST together with 5 μg of HDAC6 protein were incubated with 30 μl of glutathione Sepharose 4B in 1 ml of *in vitro* binding buffer (25 mM HEPES, pH 7.5, 100 mM KCl, 3 mM $MgCl_2$, 1 mM EDTA, 10% glycerol, 0.1% NP-40, and 1 mM DTT) at 4°C for 4 h. The beads were washed six times with *in vitro* binding buffer. Thereafter, the supernatant was discarded and the same volume of 2 × loading buffer was added into the tube. The samples were then heated at 98°C for 10 min, and the supernatant was subjected to SDS–PAGE.

In vitro deacetylation assay

HA-HDAC6 was immunoprecipitated from HEK293T cells with the anti-HA antibody. GST-IDH1 and GST-IDH1 K233R proteins were purified from HEK293T cells using Glutathione Sepharose 4B and incubated with the HA-HDAC6 immunoprecipitate in a buffer containing 25 mM Tris–HCl (pH 8.0), 50 mM NaCl, 1 mM DTT, and 5 mM NAD^+ at 37°C for 1 h. The mixture was then subjected to immunoblotting.

IDH activity assay

The IDH activity analyses were performed using the IDH Activity Assay Kit (MAK062, Sigma-Aldrich) according to the manufacturer's instructions. Briefly, NADH standards were employed to establish a standard curve. Cell samples were resuspended in 200 μl IDH assay buffer and centrifuged at 13,000 *g* for 10 min at 4°C. After centrifugation, the supernatant was transferred to a new 1.5 ml tube. Then, 42 μl of sample and 8 μl of developer were mixed and added into a well of a 96-well plate. In the meantime, 38 μl of sample, 8 μl of developer, 2 μl of substrate, and 2 μl of $NADP^+$ were mixed thoroughly and added into a well of a 96-well plate. The plate was incubated at 37°C for 3 min and the absorbance was spectrophotometrically measured at 450 nm, referred to as $T_{initial}$. The absorbance was measured every 5 min until the final value was higher than the value of the standard NADH sample

with the maximum concentration, and the value obtained just below the maximum value of standard NADH was referred to as T_{final}. The relative IDH activity of each sample was then calculated.

α-KG detection

The α-KG level was measured using the Alpha Ketoglutarate Assay Kit (ab83431, Abcam) according to the manufacturer's instructions. Briefly, the standard curve was established by α-KG standard samples. Cells were suspended in the α-KG assay buffer and centrifuged at 13,000 *g* for 5 min at 4°C. After centrifugation, the supernatant was transferred to a new tube. Perchloric acid was then added for deproteinization. After adjustment of the pH to 7.5 with KOH, the sample was centrifuged at 13,000 *g* for 15 min at 4°C and the supernatant was used for detection. To examine the α-KG level, α-KG converting enzyme, α-KG enzyme mix, and α-KG probe were added to the 96-well plate containing the α-KG assay buffer and incubated at 37°C for 30 min in the dark. Absorbance was then measured by spectrophotometry at 570 nm.

Bioinformatics analysis

Trimmed reads were mapped to the mouse reference genome (GRCm39) using Hisat2 (Love *et al*, 2014; Kim *et al*, 2015). Gene expression levels were quantified as fragments per kilobase per million mapped reads (FPKM), which was calculated using featurecounts (Liao *et al*, 2014). DESeq2 (Love *et al*, 2014) was used to perform differential gene expression analyses between samples. Heatmap was generated using the function "pheatmap" in R packages, and correlation coefficients were calculated using the function "cor" in R (Version 4.1.1). Volcano plot was generated using the "ggplot2" package. P-value < 0.05, $\log_2$FoldChange > 1 and $\log_2$FoldChange < −1 were set as the threshold for DEG analyses. Visualization of hydroxymethylation results was performed using IGV (version 2.16.1). The genome-wide distribution of 5hmC was visualized using Circos (Krzywinski *et al*, 2009).

qPCR

Total RNAs were extracted with the Trizol reagent (15596018, Thermo Fisher Scientific), and then converted into cDNAs using M-MLV reverse transcriptase (M1701, Promega, Wisconsin, USA). Gene expression analysis was performed using FastStart Universal SYBR Green Master (Rox; 04913914001, Roche).

Statistical analysis

All statistical data were analyzed with Prism (GraphPad) and presented as mean ± SEM. Statistical significance was determined by the Student's *t*-test for comparison between two groups and by the one-way ANOVA test for multiple comparisons. *P*-values less than 0.05 were considered statistically significant.

Data availability

The oxBS-seq and RNA-seq datasets produced in this study are available in the following databases:

- oxBS-seq: GSE234147 (https://www.ncbi.nlm.nih.gov/geo/query/acc.cgi?acc=GSE234147).
- RNA-seq: GSE203239 (https://www.ncbi.nlm.nih.gov/geo/query/acc.cgi?acc=GSE203239).

Expanded View for this article is available online.

Acknowledgements
We thank Dr. Lingyi Chen and Dr. Jiaxi Zhou for discussion and Dr. Tso-Pang Yao for providing *Hdac6* knockout mice. This work was supported by grants from the National Key R&D Program of China (2021YFA1101001 to JZ), National Natural Science Foundation of China (32070647 to CX, 32100656 to XD, 31970749 to LS, and 32100614 to YW), Key Projects of Tianjin Applied Basic Research Diversified Investment Foundation (21JCZDJC01020 to CX), and Haihe Laboratory of Cell Ecosystem (22HHXBJC00001 to JZ).

Author contributions
Jia Yang: Conceptualization; resources; data curation; formal analysis; validation; investigation; visualization; methodology; writing – original draft. **Yang Liu:** Conceptualization; resources; data curation; formal analysis; validation; investigation; visualization; methodology; writing – original draft. **Hanxiao Yin:** Data curation; formal analysis; investigation; visualization. **Songbo Xie:** Data curation; formal analysis; investigation; visualization. **Linlin Zhang:** Data curation; formal analysis; investigation; visualization. **Xifeng Dong:** Data curation; formal analysis; funding acquisition; investigation; visualization. **Hua Ni:** Data curation; formal analysis; investigation; visualization. **Weiwen Bu:** Data curation; formal analysis; investigation; visualization. **Hongbo Ma:** Data curation; formal analysis; investigation; visualization. **Peng Liu:** Data curation; formal analysis; investigation; visualization. **Haiyan Zhu:** Data curation; formal analysis; investigation; visualization. **Rongxia Guo:** Data curation; formal analysis; investigation; visualization. **Lei Sun:** Data curation; formal analysis; funding acquisition; investigation; visualization. **Yue Wu:** Data curation; formal analysis; funding acquisition; investigation; visualization. **Juan Qin:** Data curation; formal analysis; investigation; visualization. **Baofa Sun:** Visualization. **Dengwen Li:** Resources. **Hongbo R Luo:** Resources. **Min Liu:** Writing – review and editing. **Chenghao Xuan:** Conceptualization; supervision; funding acquisition; validation; methodology; project administration; writing – review and editing. **Jun Zhou:** Conceptualization; data curation; formal analysis; supervision; funding acquisition; investigation; methodology; project administration; writing – review and editing.

Disclosure and competing interests statement
The authors declare that they have no conflict of interest.

References

Butler KV, Kalin J, Brochier C, Vistoli G, Langley B, Kozikowski AP (2010) Rational design and simple chemistry yield a superior, neuroprotective HDAC6 inhibitor, tubastatin A. *J Am Chem Soc* 132: 10842–10846

Challen GA, Sun D, Jeong M, Luo M, Jelinek J, Berg JS, Bock C, Vasanthakumar A, Gu H, Xi Y *et al* (2011) Dnmt3a is essential for hematopoietic stem cell differentiation. *Nat Genet* 44: 23–31

Chen Z, Guo Q, Song G, Hou Y (2022) Molecular regulation of hematopoietic stem cell quiescence. *Cell Mol Life Sci* 79: 218

Crisafulli L, Ficara F (2022) Micro-RNAs: a safety net to protect hematopoietic stem cell self-renewal. *Wiley Interdiscip Rev RNA* 13: e1693

Dai W, Wang Z, Wang QA, Chan D, Jiang L (2022) Metabolic reprogramming in the OPA1-deficient cells. *Cell Mol Life Sci* 79: 517

Dang L, White DW, Gross S, Bennett BD, Bittinger MA, Driggers EM, Fantin VR, Jang HG, Jin S, Keenan MC *et al* (2009) Cancer-associated IDH1 mutations produce 2-hydroxyglutarate. *Nature* 462: 739 – 744

Dhoke NR, Kalabathula E, Kaushik K, Geesala R, Sravani B, Das A (2016) Histone deacetylases differentially regulate the proliferative phenotype of mouse bone marrow stromal and hematopoietic stem/progenitor cells. *Stem Cell Res* 17: 170 – 180

Elizalde C, Fernandez-Rueda J, Salcedo JM, Dorronsoro A, Ferrin I, Jakobsson E, Trigueros C (2012) Histone deacetylase 3 modulates the expansion of human hematopoietic stem cells. *Stem Cells Dev* 21: 2581 – 2591

Essers MA, Offner S, Blanco-Bose WE, Waibler Z, Kalinke U, Duchosal MA, Trumpp A (2009) IFNalpha activates dormant haematopoietic stem cells in vivo. *Nature* 458: 904 – 908

Ferrari G, Thrasher AJ, Aiuti A (2021) Gene therapy using haematopoietic stem and progenitor cells. *Nat Rev Genet* 22: 216 – 234

Figueroa ME, Abdel-Wahab O, Lu C, Ward PS, Patel J, Shih A, Li Y, Bhagwat N, Vasanthakumar A, Fernandez HF *et al* (2010) Leukemic IDH1 and IDH2 mutations result in a hypermethylation phenotype, disrupt TET2 function, and impair hematopoietic differentiation. *Cancer Cell* 18: 553 – 567

Geisbrecht BV, Gould SJ (1999) The human PICD gene encodes a cytoplasmic and peroxisomal NADP(+)-dependent isocitrate dehydrogenase. *J Biol Chem* 274: 30527 – 30533

Gross S, Cairns RA, Minden MD, Driggers EM, Bittinger MA, Jang HG, Sasaki M, Jin S, Schenkein DP, Su SM *et al* (2010) Cancer-associated metabolite 2-hydroxyglutarate accumulates in acute myelogenous leukemia with isocitrate dehydrogenase 1 and 2 mutations. *J Exp Med* 207: 339 – 344

Guo H, Friedman AD (2011) Phosphorylation of RUNX1 by cyclin-dependent kinase reduces direct interaction with HDAC1 and HDAC3. *J Biol Chem* 286: 208 – 215

Haggarty SJ, Koeller KM, Wong JC, Grozinger CM, Schreiber SL (2003) Domain-selective small-molecule inhibitor of histone deacetylase 6 (HDAC6)-mediated tubulin deacetylation. *Proc Natl Acad Sci USA* 100: 4389 – 4394

Hubbert C, Guardiola A, Shao R, Kawaguchi Y, Ito A, Nixon A, Yoshida M, Wang XF, Yao TP (2002) HDAC6 is a microtubule-associated deacetylase. *Nature* 417: 455 – 458

Huo L, Li D, Sun X, Shi X, Karna P, Yang W, Liu M, Qiao W, Aneja R, Zhou J (2011) Regulation of Tat acetylation and transactivation activity by the microtubule-associated deacetylase HDAC6. *J Biol Chem* 286: 9280 – 9286

Izzo F, Lee SC, Poran A, Chaligne R, Gaiti F, Gross B, Murali RR, Deochand SD, Ang C, Jones PW *et al* (2020) DNA methylation disruption reshapes the hematopoietic differentiation landscape. *Nat Genet* 52: 378 – 387

Jiang L, Shestov AA, Swain P, Yang C, Parker SJ, Wang QA, Terada LS, Adams ND, McCabe MT, Pietrak B *et al* (2016) Reductive carboxylation supports redox homeostasis during anchorage-independent growth. *Nature* 532: 255 – 258

Jiang P, Wang H, Zheng J, Han Y, Huang H, Qian P (2019) Epigenetic regulation of hematopoietic stem cell homeostasis. *Blood Sci* 1: 19 – 28

Kalaszczynska I, Geng Y, Iino T, Mizuno S, Choi Y, Kondratiuk I, Silver DP, Wolgemuth DJ, Akashi K, Sicinski P (2009) Cyclin A is redundant in fibroblasts but essential in hematopoietic and embryonic stem cells. *Cell* 138: 352 – 365

Kaluza D, Kroll J, Gesierich S, Yao TP, Boon RA, Hergenreider E, Tjwa M, Rossig L, Seto E, Augustin HG *et al* (2011) Class IIb HDAC6 regulates endothelial cell migration and angiogenesis by deacetylation of cortactin. *EMBO J* 30: 4142 – 4156

Karatepe K, Zhu H, Zhang X, Guo R, Kambara H, Loison F, Liu P, Yu H, Ren Q, Luo X *et al* (2018) Proteinase 3 limits the number of hematopoietic stem and progenitor cells in murine bone marrow. *Stem Cell Reports* 11: 1092 – 1105

Kerenyi MA, Shao Z, Hsu YJ, Guo G, Luc S, O'Brien K, Fujiwara Y, Peng C, Nguyen M, Orkin SH (2013) Histone demethylase Lsd1 represses hematopoietic stem and progenitor cell signatures during blood cell maturation. *Elife* 2: e00633

Khalaj M, Woolthuis CM, Hu W, Durham BH, Chu SH, Qamar S, Armstrong SA, Park CY (2017) miR-99 regulates normal and malignant hematopoietic stem cell self-renewal. *J Exp Med* 214: 2453 – 2470

Kilgore M, Miller CA, Fass DM, Hennig KM, Haggarty SJ, Sweatt JD, Rumbaugh G (2010) Inhibitors of class 1 histone deacetylases reverse contextual memory deficits in a mouse model of Alzheimer's disease. *Neuropsychopharmacology* 35: 870 – 880

Kim YM, Hwang S, Kim YM, Pyun BJ, Kim TY, Lee ST, Gho YS, Kwon YG (2002) Endostatin blocks vascular endothelial growth factor-mediated signaling via direct interaction with KDR/Flk-1. *J Biol Chem* 277: 27872 – 27879

Kim D, Langmead B, Salzberg SL (2015) HISAT: a fast spliced aligner with low memory requirements. *Nat Methods* 12: 357 – 360

Ko M, Bandukwala HS, An J, Lamperti ED, Thompson EC, Hastie R, Tsangaratou A, Rajewsky K, Koralov SB, Rao A (2011) Ten-Eleven-Translocation 2 (TET2) negatively regulates homeostasis and differentiation of hematopoietic stem cells in mice. *Proc Natl Acad Sci USA* 108: 14566 – 14571

Kozar K, Ciemerych MA, Rebel VI, Shigematsu H, Zagozdzon A, Sicinska E, Geng Y, Yu Q, Bhattacharya S, Bronson RT *et al* (2004) Mouse development and cell proliferation in the absence of D-cyclins. *Cell* 118: 477 – 491

Krzywinski M, Schein J, Birol I, Connors J, Gascoyne R, Horsman D, Jones SJ, Marra MA (2009) Circos: an information aesthetic for comparative genomics. *Genome Res* 19: 1639 – 1645

Laurenti E, Gottgens B (2018) From haematopoietic stem cells to complex differentiation landscapes. *Nature* 553: 418 – 426

Li D, Xie S, Ren Y, Huo L, Gao J, Cui D, Liu M, Zhou J (2011) Microtubule-associated deacetylase HDAC6 promotes angiogenesis by regulating cell migration in an EB1-dependent manner. *Protein Cell* 2: 150 – 160

Liao Y, Smyth GK, Shi W (2014) featureCounts: an efficient general purpose program for assigning sequence reads to genomic features. *Bioinformatics* 30: 923 – 930

Lio CJ, Yuita H, Rao A (2019) Dysregulation of the TET family of epigenetic regulators in lymphoid and myeloid malignancies. *Blood* 134: 1487 – 1497

Liu JY, Qian D, He LR, Li YH, Liao YJ, Mai SJ, Tian XP, Liu YH, Zhang JX, Kung HF *et al* (2013) PinX1 suppresses bladder urothelial carcinoma cell proliferation via the inhibition of telomerase activity and p16/cyclin D1 pathway. *Mol Cancer* 12: 148

Love MI, Huber W, Anders S (2014) Moderated estimation of fold change and dispersion for RNA-seq data with DESeq2. *Genome Biol* 15: 550

Mahadik B, Hannon B, Harley BAC (2019) A computational model of feedback-mediated hematopoietic stem cell differentiation in vitro. *PLoS ONE* 14: e0212502

Moran-Crusio K, Reavie L, Shih A, Abdel-Wahab O, Ndiaye-Lobry D, Lobry C, Figueroa ME, Vasanthakumar A, Patel J, Zhao X *et al* (2011) Tet2 loss leads to increased hematopoietic stem cell self-renewal and myeloid transformation. *Cancer Cell* 20: 11 – 24

Neganova ME, Klochkov SG, Aleksandrova YR, Aliev G (2022) Histone modifications in epigenetic regulation of cancer: perspectives and achieved progress. *Semin Cancer Biol* 83: 452 – 471

Ntziachristos P, Abdel-Wahab O, Aifantis I (2016) Emerging concepts of epigenetic dysregulation in hematological malignancies. *Nat Immunol* 17: 1016 – 1024

Okoye-Okafor UC, Bartholdy B, Cartier J, Gao EN, Pietrak B, Rendina AR, Rominger C, Quinn C, Smallwood A, Wiggall KJ *et al* (2015) New IDH1 mutant inhibitors for treatment of acute myeloid leukemia. *Nat Chem Biol* 11: 878 – 886

O'Reilly MS, Boehm T, Shing Y, Fukai N, Vasios G, Lane WS, Flynn E, Birkhead JR, Olsen BR, Folkman J (1997) Endostatin: an endogenous inhibitor of angiogenesis and tumor growth. *Cell* 88: 277 – 285

Ozawa Y, Towatari M, Tsuzuki S, Hayakawa F, Maeda T, Miyata Y, Tanimoto M, Saito H (2001) Histone deacetylase 3 associates with and represses the transcription factor GATA-2. *Blood* 98: 2116 – 2123

Quivoron C, Couronne L, Della Valle V, Lopez CK, Plo I, Wagner-Ballon O, Do Cruzeiro M, Delhommeau F, Arnulf B, Stern MH *et al* (2011) TET2 inactivation results in pleiotropic hematopoietic abnormalities in mouse and is a recurrent event during human lymphomagenesis. *Cancer Cell* 20: 25 – 38

Ran J, Yang Y, Li D, Liu M, Zhou J (2015) Deacetylation of alpha-tubulin and cortactin is required for HDAC6 to trigger ciliary disassembly. *Sci Rep* 5: 12917

Ran J, Liu M, Feng J, Li H, Ma H, Song T, Cao Y, Zhou P, Wu Y, Yang Y *et al* (2020) ASK1-mediated phosphorylation blocks HDAC6 ubiquitination and degradation to drive the disassembly of photoreceptor connecting cilia. *Dev Cell* 53: 287 – 299

Ran J, Zhang Y, Zhang S, Li H, Zhang L, Li Q, Qin J, Li D, Sun L, Xie S *et al* (2022) Targeting the HDAC6-cilium axis ameliorates the pathological changes associated with retinopathy of prematurity. *Adv Sci (Weinh)* 9: e2105365

Rasheed A (2022) Niche regulation of hematopoiesis: the environment is "Micro", but the influence is large. *Arterioscler Thromb Vasc Biol* 42: 691 – 699

Rasmussen KD, Berest I, Kebetaler S, Nishimura K, Simon-Carrasco L, Vassiliou GS, Pedersen MT, Christensen J, Zaugg JB, Helin K (2019) TET2 binding to enhancers facilitates transcription factor recruitment in hematopoietic cells. *Genome Res* 29: 564 – 575

Reya T, Duncan AW, Ailles L, Domen J, Scherer DC, Willert K, Hintz L, Nusse R, Weissman IL (2003) A role for Wnt signalling in self-renewal of haematopoietic stem cells. *Nature* 423: 409 – 414

Rodrigues CP, Shvedunova M, Akhtar A (2020) Epigenetic regulators as the gatekeepers of hematopoiesis. *Trends Genet* 37: 125 – 142

Sasaki M, Knobbe CB, Munger JC, Lind EF, Brenner D, Brustle A, Harris IS, Holmes R, Wakeham A, Haight J *et al* (2012) IDH1(R132H) mutation increases murine haematopoietic progenitors and alters epigenetics. *Nature* 488: 656 – 659

Sealy L, Chalkley R (1978) The effect of sodium butyrate on histone modification. *Cell* 14: 115 – 121

Sezaki M, Hayashi Y, Wang Y, Johansson A, Umemoto T, Takizawa H (2020) Immuno-modulation of hematopoietic stem and progenitor cells in inflammation. *Front Immunol* 11: 585367

Shi X, He BL, Ma AC, Guo Y, Chi Y, Man CH, Zhang W, Zhang Y, Wen Z, Cheng T *et al* (2015) Functions of idh1 and its mutation in the regulation of developmental hematopoiesis in zebrafish. *Blood* 125: 2974 – 2984

Shi DQ, Ali I, Tang J, Yang WC (2017) New insights into 5hmC DNA modification: generation, distribution and function. *Front Genet* 8: 100

Tahiliani M, Koh KP, Shen Y, Pastor WA, Bandukwala H, Brudno Y, Agarwal S, Iyer LM, Liu DR, Aravind L *et al* (2009) Conversion of 5-methylcytosine to 5-hydroxymethylcytosine in mammalian DNA by MLL partner TET1. *Science* 324: 930 – 935

Thol F, Weissinger EM, Krauter J, Wagner K, Damm F, Wichmann M, Gohring G, Schumann C, Bug G, Ottmann O *et al* (2010) IDH1 mutations in patients with myelodysplastic syndromes are associated with an unfavorable prognosis. *Haematologica* 95: 1668 – 1674

Tian XP, Jin XH, Li M, Huang WJ, Xie D, Zhang JX (2017) The depletion of PinX1 involved in the tumorigenesis of non-small cell lung cancer promotes cell proliferation via p15/cyclin D1 pathway. *Mol Cancer* 16: 74

Tsukada Y, Fang J, Erdjument-Bromage H, Warren ME, Borchers CH, Tempst P, Zhang Y (2006) Histone demethylation by a family of JmjC domain-containing proteins. *Nature* 439: 811 – 816

Valenzuela-Fernandez A, Alvarez S, Gordon-Alonso M, Barrero M, Ursa A, Cabrero JR, Fernandez G, Naranjo-Suarez S, Yanez-Mo M, Serrador JM *et al* (2005) Histone deacetylase 6 regulates human immunodeficiency virus type 1 infection. *Mol Biol Cell* 16: 5445 – 5454

Van Kanegan MJ, Strack S (2009) The protein phosphatase 2A regulatory subunits B'beta and B'delta mediate sustained TrkA neurotrophin receptor autophosphorylation and neuronal differentiation. *Mol Cell Biol* 29: 662 – 674

Verdel A, Curtet S, Brocard MP, Rousseaux S, Lemercier C, Yoshida M, Khochbin S (2000) Active maintenance of mHDA2/mHDAC6 histone-deacetylase in the cytoplasm. *Curr Biol* 10: 747 – 749

Walker L, Lynch M, Silverman S, Fraser J, Boulter J, Weinmaster G, Gasson JC (1999) The Notch/Jagged pathway inhibits proliferation of human hematopoietic progenitors in vitro. *Stem Cells* 17: 162 – 171

Wang D, Meng Q, Huo L, Yang M, Wang L, Chen X, Wang J, Li Z, Ye X, Liu N *et al* (2015) Overexpression of Hdac6 enhances resistance to virus infection in embryonic stem cells and in mice. *Protein Cell* 6: 152 – 156

Weissman IL (2000) Stem cells: units of development, units of regeneration, and units in evolution. *Cell* 100: 157 – 168

Wilkinson AC, Igarashi KJ, Nakauchi H (2020) Haematopoietic stem cell self-renewal in vivo and ex vivo. *Nat Rev Genet* 21: 541 – 554

Wu X, Zhang Y (2017) TET-mediated active DNA demethylation: mechanism, function and beyond. *Nat Rev Genet* 18: 517 – 534

Wu X, Li G, Xie R (2018) Decoding the role of TET family dioxygenases in lineage specification. *Epigenetics Chromatin* 11: 58

Xie S, Zhang L, Dong D, Ge R, He Q, Fan C, Xie W, Zhou J, Li D, Liu M (2020) HDAC6 regulates antibody-dependent intracellular neutralization of viruses via deacetylation of TRIM21. *J Biol Chem* 295: 14343 – 14351

Xu X, Zhao J, Xu Z, Peng B, Huang Q, Arnold E, Ding J (2004) Structures of human cytosolic NADP-dependent isocitrate dehydrogenase reveal a novel self-regulatory mechanism of activity. *J Biol Chem* 279: 33946 – 33957

Xu W, Yang H, Liu Y, Yang Y, Wang P, Kim SH, Ito S, Yang C, Wang P, Xiao MT *et al* (2011) Oncometabolite 2-hydroxyglutarate is a competitive inhibitor of alpha-ketoglutarate-dependent dioxygenases. *Cancer Cell* 19: 17 – 30

Xu C, Ooi WF, Qamra A, Tan J, Chua BY, Ho SWT, Das K, Adam Isa ZF, Li Z, Yao X *et al* (2020) HNF4alpha pathway mapping identifies wild-type IDH1 as a targetable metabolic node in gastric cancer. *Gut* 69: 231 – 242

Yan B, Liu Y, Bai H, Chen M, Xie S, Li D, Liu M, Zhou J (2017) HDAC6 regulates IL-17 expression in T lymphocytes: implications for HDAC6-targeted therapies. *Theranostics* 7: 1002 – 1009

Yan B, Xie S, Liu Y, Liu W, Li D, Liu M, Luo HR, Zhou J (2018) Histone deacetylase 6 modulates macrophage infiltration during inflammation. *Theranostics* 8: 2927 – 2938

Yoshida M, Kijima M, Akita M, Beppu T (1990) Potent and specific inhibition of mammalian histone deacetylase both in vivo and in vitro by trichostatin A. *J Biol Chem* 265: 17174 – 17179

Zhang Y, Li N, Caron C, Matthias G, Hess D, Khochbin S, Matthias P (2003) HDAC-6 interacts with and deacetylates tubulin and microtubules in vivo. *EMBO J* 22: 1168 – 1179

Zhang X, Yuan Z, Zhang Y, Yong S, Salas-Burgos A, Koomen J, Olashaw N, Parsons JT, Yang XJ, Dent SR *et al* (2007) HDAC6 modulates cell motility by altering the acetylation level of cortactin. *Mol Cell* 27: 197 – 213

Zhang L, Liu S, Liu N, Zhang Y, Liu M, Li D, Seto E, Yao TP, Shui W, Zhou J (2015) Proteomic identification and functional characterization of MYH9, Hsc70, and DNAJA1 as novel substrates of HDAC6 deacetylase activity. *Protein Cell* 6: 42 – 54

Zhang X, Su J, Jeong M, Ko M, Huang Y, Park HJ, Guzman A, Lei Y, Huang YH, Rao A *et al* (2016) DNMT3A and TET2 compete and cooperate to repress lineage-specific transcription factors in hematopoietic stem cells. *Nat Genet* 48: 1014 – 1023

